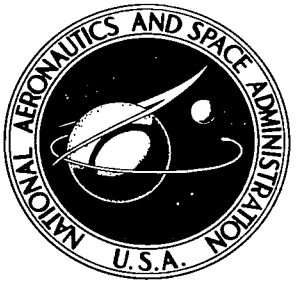

DESIGN CHARTS FOR ARBITRARILY PIVOTED, LIQUID-LUBRICATED, FLAT-SECTOR-PAD THRUST BEARING

Izhak Etsion

Lewis Research Center
Cleveland, Ohio 44135

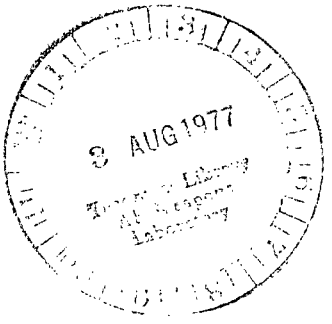

NATIONAL AERONAUTICS AND SPACE ADMINISTRATION • WASHINGTON, D. C. • JULY 1977

1. Report No. NASA TN D-8344	2. Government Accession No.	3. Recipient's Catalog No.
4. Title and Subtitle DESIGN CHARTS FOR ARBITRARILY PIVOTED, LIQUID-LUBRICATED, FLAT-SECTOR-PAD THRUST BEARING		5. Report Date July 1977 6. Performing Organization Code
7. Author(s) Izhak Etsion		8. Performing Organization Report No. E-8899
9. Performing Organization Name and Address Lewis Research Center National Aeronautics and Space Administration Cleveland, Ohio 44135		10. Work Unit No. 505-04 11. Contract or Grant No.
12. Sponsoring Agency Name and Address National Aeronautics and Space Administration Washington, D.C. 20546		13. Type of Report and Period Covered Technical Note 14. Sponsoring Agency Code
15. Supplementary Notes		

16. Abstract

A flat, sector-shaped geometry for a liquid-lubricated thrust bearing is analyzed considering both the pitch and roll of the pad. Results are presented in design charts that enable a direct approach to the design of point- and line-pivoted, tilting pad bearings. A comparison is made with the Michell bearing approximation and it is found that this approximation always overestimates load capacity.

17. Key Words (Suggested by Author(s)) Bearings Thrust bearings	18. Distribution Statement Unclassified - unlimited STAR Category 37

19. Security Classif. (of this report) Unclassified	20. Security Classif. (of this page) Unclassified	21. No. of Pages 59	22. Price* $4.50

* For sale by the National Technical Information Service, Springfield, Virginia 22161

DESIGN CHARTS FOR ARBITRARILY PIVOTED, LIQUID-LUBRICATED, FLAT-SECTOR-PAD THRUST BEARING

by Izhak Etsion*

Lewis Research Center

SUMMARY

A flat, sector-shaped geometry for a liquid-lubricated thrust bearing is analyzed considering both the pitch and roll of the pad. Performance characteristics such as center-of-pressure location, unit load, friction loss coefficient, and lubricant flow are presented in design charts. These charts enable a direct approach to the design of both point- and line-pivoted pads and also provide the necessary procedures for the design of nontilting flat pads. The various features of point- and line-pivoted configurations are discussed, and a comparison is made with the Michell bearing approximation. It is found that this approximation always overestimates load capacity.

INTRODUCTION

Although during the last three decades the commonly used flat sector pad has been extensively analyzed, most of the investigators treated a simplified oil film shape (refs. 1 to 9). Either a linear film thickness variation was assumed in the circumferential direction, independent of the radius, or some sort of an exponential oil film shape was used. In some works (e. g., refs. 1 and 7) the sector shape is transformed into a rectangular configuration, which further distorts the actual geometry.

An actual tilting pad assumes both pitch and roll about some point and, for the flat surface, the clearance varies in both the radial and circumferential directions, with the circumferential variation being sinusoidal rather than linear. Therefore, all of the previously mentioned solutions are approximations and may lead to an overly optimistic

*National Research Council - National Aeronautics and Space Administration Research Associate.

design of a flat, sector-shaped tilting pad.

When dealing with pivoted-pad bearings it must be remembered that, in order to satisfy equilibrium of moments, the resultant of the hydrodynamic pressures must pass through the pivot. Thus, for a given pivot location, the solution of the Reynolds equation should result in a predetermined location for the center of pressure. Unfortunately, such a direct solution is impossible and the designer must presently use a tedious iteration approach (refs. 10 and 11) or select a certain pad orientation and place a point pivot at the resulting center of pressure (ref. 12). In both cases the solutions are limited to specific design points. That is, for given values of load, speed, and minimum film thickness there corresponds only one pivot location. In real applications the pivot is fixed within the pad area. Hence, when changing the operating conditions the pad must change its pitch and roll angles so that the center of pressure will always stay at the pivot location. A complete analysis of the tilting pad thrust bearing must therefore cover all the possible pitch and roll angles for possible pivot locations within the pad area. The objective of this work is to obtain such a solution to provide the necessary data for the design of flat, sector-shaped tilting pad thrust bearings. This will be presented for the incompressible case in the form of design charts that give the load capacity, friction loss, and lubricant flow for various pivot locations and pad tilt angles. The solutions are also valid for the tilting pad gas bearing at low compressibility numbers.

SYMBOLS

A pad area, $\beta\left(r_o^2 - r_i^2\right)/2$

F friction loss

$\overline{F}$ nondimensional friction loss, $F/K\omega r_o^2 h_2$

H nondimensional film thickness, h/h_p

h film thickness

K bearing parameter, $6\mu\omega(r_o/h_2)^2$

P dimensionless pressure, p/K

p pressure

Q volumetric oil flow

$\overline{Q}$ nondimensional flow, $Q/(1/2)\omega h_2 r_o^2$

R nondimensional radial coordinate, r/r_o

r radial coordinate

W pad load capacity

$\overline{W}$ nondimensional load, W/Kr_o^2

β angular extent of pad

ϵ tilt parameter, $\gamma r_o/h_p$

γ tilt about pitch line

θ angular coordinate, measured from leading edge

μ viscosity

τ shear stress

ω shaft speed

Subscripts:

cp center of pressure

i inner radius

l leading edge

o outer radius

p pitch line

t trailing edge

1 maximum film thickness

2 minimum film thickness

THEORETICAL BACKGROUND

The incompressible Reynolds equation in polar coordinates is

$$\frac{\partial}{\partial r}\left(\frac{rh^3}{\mu}\frac{\partial p}{\partial r}\right)+\frac{1}{r}\frac{\partial}{\partial \theta}\left(\frac{h^3}{\mu}\frac{\partial p}{\partial \theta}\right)=6\omega r\frac{\partial h}{\partial \theta} \tag{1}$$

In order to solve equation (1) for the pressure distribution, the oil film thickness h has to be expressed in terms of the independent variables r and θ. In an earlier report (ref. 13), it was shown that any pitch and roll of a sector-shaped pad about a certain point can be transformed to a corresponding pure pitch about a certain radial line. This radial line may or may not be located between the leading and trailing edges of the pad. This can be understood from figure 1 by visualizing a plane parallel to the runner that goes through the origin of the sector (point O in fig. 1). The radial line (called the pitch line) about which the pad motion is purely pitch is the intersection between this parallel plane and the plane of the tilted sector, and it can be either inside or outside the sector boundaries. By considering the clearance h_p along this radial pitch line as a reference, the film thickness at any point (r, θ) is given by

$$h = h_p + \gamma r \sin(\theta_p - \theta) \tag{2}$$

where γ is the amount of tilt about the pitch line. If we let $p = KP$, $h = Hh_p$, and $r = Rr_o$, where $K = 6\mu\omega(r_o/h_2)^2$, equations (1) and (2) can be transformed to the dimensionless form

$$\frac{\partial}{\partial R}\left(RH^3 \frac{\partial P}{\partial R}\right) + \frac{1}{R}\frac{\partial}{\partial \theta}\left(H^3 \frac{\partial P}{\partial \theta}\right) = H_2^2 R \frac{\partial H}{\partial \theta} \tag{3}$$

and

$$H = 1 + \epsilon R \sin(\theta_p - \theta) \tag{4}$$

where H_2 in equation (3) is the dimensionless minimum film thickness h_2/h_p and the tilt parameter ϵ is $\gamma(r_o/h_p)$. The boundary conditions for equation (3) are $P = 0$ along the pad boundaries.

Four parameters are needed to determine a unique solution of equation (3): the radius ratio r_i/r_o, the pad angular extent β, the radial pitch line location θ_p, and the tilt parameter ϵ. Equation (3) is expanded by finite differences and solved numerically by using the Gauss-Seidel iteration method (ref. 14). After the pressure distribution is known, the total load capacity is obtained from

$$\overline{W} = \frac{W}{Kr_o^2} = \int_{r_i/r_o}^{1} \int_0^{\beta} PR \, d\theta \, dR \tag{5}$$

The pad area is given by

$$A = \frac{\beta r_o^2}{2}\left[1 - \left(\frac{r_i}{r_o}\right)^2\right]$$

and the dimensionless unit load of the bearing is

$$\frac{W}{KA} = \frac{2\overline{W}}{\beta\left[1 - \left(\frac{r_i}{r_o}\right)^2\right]} \tag{6}$$

The dimensionless radial and angular coordinates of the center of pressure are given by

$$R_{cp} = \frac{1}{\overline{W}} \int_{r_i/r_o}^{1} \int_0^{\beta} PR^2 \, d\theta \, dR \tag{7a}$$

and

$$\sin \theta_{cp} = \frac{1}{\overline{W} R_{cp}} \int_{r_i/r_o}^{1} \int_0^{\beta} PR^2 \sin \theta \, d\theta \, dR \tag{7b}$$

The shear stress on the runner is

$$\tau = \frac{\mu \omega r}{h} + \frac{h}{2r} \frac{\partial p}{\partial \theta}$$

and the power loss is

$$F = \int_{r_i}^{r_o} \int_0^{\beta} \tau \omega r^2 \, d\theta \, dr$$

Defining the dimensionless power loss

$$\overline{F} = \frac{F}{K \omega r_o^2 h_2}$$

gives

$$\overline{F} = \int_{r_i/r_o}^{1} \int_{0}^{\beta} \left(\frac{R^3}{6} \frac{H_2}{H} + \frac{R}{2} \frac{H}{H_2} \frac{\partial P}{\partial \theta} \right) d\theta \, dR \tag{8}$$

The circumferential volumetric flow is obtained from

$$\overline{Q} = \frac{Q}{\frac{1}{2} \omega r_o^2 h_2} = \int_{r_i/r_o}^{1} \left[\frac{H}{H_2} R - \left(\frac{H}{H_2} \right)^3 \frac{1}{R} \frac{\partial P}{\partial \theta} \right] dR \tag{9}$$

When evaluating the integral at $\theta = 0$, equation (9) gives the inflow $\overline{Q}_l$ across the leading edge. At $\theta = \beta$ the outflow $\overline{Q}_t$ across the trailing edge is obtained.

RESULTS AND DISCUSSION

In total, 12 different geometries were analyzed. Inner to outer radius ratios were 0.3, 0.5, and 0.7 at pad angles of 30^o, 45^o, 60^o, and 90^o. Each pad was run at various tilt parameters and pitch line locations. A modified tilt parameter in the form $\gamma r_o/h_2$ was used as the basis for calculations since the minimum film thickness h_2 rather than h_p is of importance to the designer. The pitch line location θ_p was restricted to the range $\beta - \pi/2 < \theta_p < \pi/2$. This assures a circumferentially converging film thickness all over the pad area (ref. 13) and eliminates the possibility of cavitation.

Figure 2 is a summary of results for the maximum available unit load that can be obtained at various pitch line locations. It is clear that for the whole range of pad geometries there is a sharp maximum at $\theta_p/\beta = 1$. Hence, to obtain the maximum load capacity from a given pad, the pad should be tilted in a way that maintains a uniform minimum film thickness along its trailing edge.

A physical explanation for this is that the pressure buildup in the lubricating film is affected by the resistance to lubricant outflow. Some of this flow occurs along the inner and outer circumferences of the pad, but the larger portion leaks across the trailing edge. Hence, it would be advantageous to decrease the escape area along this boundary. For a given minimum film thickness h_2, the least escape area and hence the highest pressure buildup can be achieved by maintaining uniform h_2 along the trailing edge.

As can be seen from figure 2, the load capacity drops sharply as θ_p exceeds β.

Therefore, it was found reasonable to limit the range of θ_p to $\theta_p/\beta = 1$. In that case the minimum film thickness, for any $\pi/2 - \beta < \theta_p < \beta$, is at the point (r_o, β), and its dimensionless value is given by

$$H_2 = 1 + \epsilon \sin(\theta_p - \beta) \tag{10}$$

The modified tilt parameter given by

$$\frac{\gamma r_o}{h_2} = \frac{\epsilon}{H_2}$$

is therefore related to ϵ through

$$\frac{\gamma r_o}{h_2} = \frac{\epsilon}{1 + \epsilon \sin(\theta_p - \beta)} \tag{11}$$

The design data for nine of the configurations are presented in figures 3 to 11 in groups of five charts for each pad geometry. In each figure, part (a) gives the center-of-pressure location for various constant values of $\gamma r_o/h_2$ and θ_p/β. Parts (b), (c), (d), and (e) give the unit load, power loss coefficient, inflow, and outflow, respectively, as functions of $\gamma r_o/h_2$ for various constant values of θ_p/β.

Use of Design Charts

Pivoted-pad bearings. - The design charts can be used for both point-pivoted and line-pivoted tilting pads. They can be used either to determine minimum film thickness for a specified load, speed, and pivot location or to find the pivot location for a given load, speed, and optimum minimum film thickness. The first approach is useful when designing for a special purpose, like a centrally pivoted pad, or when the operating conditions, like speed or load, are changed after a pivot location has been selected for a certain design point. The second approach is used when designing for specified operating conditions or for optimization purposes. In this case, for a given pad geometry, the designer selects the optimum value he wants from either part (b), (c), (d), or (e). By this selection a set of the parameters $\gamma r_o/h_2$ and θ_p/β is obtained, which, by part (a), determines the center of pressure that is identical to the pivot location. On the other hand, if the pivot location is known, the procedure is simply reversed. From part (a) for each pivot location there corresponds a set of the parameters $\gamma r_o/h_2$ and θ_p/β. For this set of parameters the dimensionless unit load

is found from part (b) in the form $Wh_2^2/6\mu\omega r_o^2 A$. Now for any given load and speed the minimum film thickness h_2 is obtained and then the tilt γ can be found from the known tilt parameter $\gamma r_o/h_2$. The friction loss F, inflow Q_l, and outflow Q_t can be found by using parts (c), (d), and (e).

With point-pivoted pads the design is straightforward. Once the pivot point is fixed, the pad alines itself by pitching and rolling, about the pivot, to obtain the necessary tilt γ about the radial line at the proper angle θ_p/β. However, when line-pivoted pads are designed, the line pivot must go through the center of pressure and be parallel to the pitch line at the angle θ_p measured from the leading edge. This assures equal performance of the line- and point-pivoted pads. For the highest load capacity and lowest friction loss the line pivot should be parallel to the trailing edge ($\theta_p/\beta = 1$). With nonradial line pivots this is not a problem at all, but with a radial line pivot the design is limited to those cases where lines of constant θ_p/β in part (a) intersect lines of constant angular center-of-pressure coordinate, $\theta_{cp}/\beta = \theta_p/\beta$. This assures equilibrium of moments about the radial line pivot. From the various parts (a) of figures 3 to 11 it can be seen that this demand makes the radial line-pivoted pad inferior to the point-pivoted one. A radial line pivot design eliminates one degree of freedom (pad roll) and fixes the radial location of the center of pressure (parts (a)). Thus the design for maximum unit load, where the desired θ_p/β is 1 and θ_{cp}/β is always less than 1, is impossible with a radial line-pivoted pad.

Another special design is that of a centrally pivoted pad. Again from parts (a) it is seen that a flat, sector pad tilted about its mid-angular line cannot produce any load capacity. The fact that such a bearing does carry load in a real application is attributed to thermal and mechanical distortions, but the efficiency of such a design is still questionable when compared with the centrally point-pivoted pad. With the point pivot, it can be seen from parts (a) and (b) that an angular location of $\theta_{cp}/\beta = 0.5$ is a viable design for a flat sector pad. More than that, for this angular location the designer can choose the optimum radial coordinate of the pivot that will maximize the unit load. This, in turn, results in the largest minimum film thickness for a given speed and load.

When a centrally pivoted, flat, sector pad is used, the penalty in unit load as compared with a design for maximum unit load is quite high. As an example, for a pad radius ratio r_i/r_o of 0.5 and angular extent β of 45^o the loss in unit load is almost 60 percent. That means a reduction of about 35 percent in minimum film thickness as compared with an optimum design for the same load and speed.

Tapered-land bearings. - The information that is contained in figures 3 to 11 is also useful for nonpivoting (fixed), flat, sector-shaped pads. For any desired operating condition, one can select a set of pitch line location θ_p/β and tilt parameter

$\gamma r_o/h_2$. Hence, the necessary taper γ can be obtained which, together with the location θ_p/β, completely defines the sector pad shape. Determining the minimum film thickness h_2 for a nonpivoting pad at off-design points involves some cross plotting. In contrast to the tilting pad, the slope γ of the nontilting pad is fixed while the center of pressure is free to change. Hence, since the parameter θ_p/β is fixed too, for any given load and speed there corresponds a different value of $\gamma r_o/h_2$. A design curve can be constructed from part (b) for any line of constant θ_p/β by multiplying values of $Wh_2^2/6\mu\omega r_o^2 A$ by their corresponding values of $(\gamma r_o/h_2)^2$. This enables one to plot the curve of $W\gamma^2/6\mu\omega A$ against the parameter $\gamma r_o/h_2$ for the line of constant θ_p/β. Now since γ is known for the fixed pad, one can find from that curve the value of $\gamma r_o/h_2$ that corresponds to any given load and speed and therefore obtain the corresponding value of h_2.

Comparison with Michell Bearing Approximation

As was mentioned in the INTRODUCTION, a common practice in tilting pad design is to approximate the oil film shape by a uniform taper in the circumferential direction. This type of bearing, where h is independent of r and varies linearly with θ, is known as the Michell bearing. In order to check the accuracy of the Michell bearing approximation, the results of reference 6 were transformed to the same dimensionless form and compared with the results of the present work. Table I presents the dimensionless unit load W/KA for various maximum to minimum film thickness ratios. Two extreme configurations were chosen for the comparison. The first sector has a low radius ratio of 1/3 and large angle of 80°, while the second sector has a radius ratio of 2/3 and an angle of 30°. From table I it is clear that the Michell bearing approximation overestimates significantly the load of an actual flat configuration. The overestimation ranges from 13 percent at $h_1/h_2 = 2$, $r_i/r_o = 2/3$, $\beta = 30^\circ$, and $\theta_p/\beta = 1$ to 170 percent at $h_1/h_2 = 9$, $r_i/r_o = 1/3$, $\beta = 80^\circ$, and $\theta_p/\beta = 0.5$.

CONCLUDING REMARKS

The pitch and roll of a sector pad about any point can be transformed to a pure pitch about some radial line. This transformation enables bearing performance to be presented as a function of only two dimensionless parameters, namely, the tilt parameter and the radial line location. This in turn provides a direct approach to the design of flat, sector-shpaed, tilting pad bearings by eliminating the need of tedious iterations.

Numerical solutions for nine different sector pads having radius ratios of 0.3, 0.5,

and 0.7 and sector angles of 30°, 45°, and 60° were obtained. Their performances are presented in design charts that enable the design of both point- and line-pivoted tilting pad bearings.

Point-pivoted pads are superior to radial-line-pivoted ones since they have an additional degree of freedom. Special designs, like the one for maximum unit load or that of a centrally pivoted pad, can be accomplished with a point-pivoted flat configuration but not with a radial-line-pivoted one.

The Michell bearing approximation, commonly used for design purposes, is unsafe since it always overestimates the load-carrying capacity of an actual flat sector pad.

Lewis Research Center,
National Aeronautics and Space Administration,
Cleveland, Ohio, September 7, 1976,
505-04.

REFERENCES

1. Brand, R. S.: The Hydrodynamic Lubrication of Sector-Shaped Pads. Trans. ASME, vol. 73, no. 11, Nov. 1951, pp. 1061-1063.

2. Charnes, A.; Saibel, E.; and Ying, A. S. C.: On the Solution of the Reynolds Equation for Slider-Bearing Lubrication. V - The Sector Thrust Bearing. Trans. ASME, vol. 75, no. 8, Aug. 1953, pp. 1125-1132.

3. Kettleborough, C. F.; Dudley, B. R.; and Baildon, E.: Michell Bearing Lubrication, Parts 1 and 2. Proc. Inst. Mech. Eng., vol. 169, 1955, pp. 746-765.

4. Sternlicht, B.; and Sneck, H. J.: Numerical Solution of Reynolds Equation for Sector Thrust Bearings. Lubr. Eng., vol. 13, no. 8, Aug. 1957, pp. 459-463.

5. Kunin, I. A.: On the Hydrodynamic Theory of Lubrication of Pad Type Bearings. Wear, vol. 2, 1958, pp. 9-20.

6. Pinkus, O.: Solution of the Tapered Land Sector Thrust Bearing. Trans. ASME, vol. 80, no. 10, Oct. 1958, pp. 1510-1516.

7. Bosma, R.; and Moes, H.: Design Charts for Optimum Bearing Configuration: 2 - The Pivoted-Pad Thrust Bearing. J. Lubr. Technol., Trans. ASME, ser. F, vol. 92, no. 4, Oct. 1970, pp. 572-577.

8. D'yackhov, A. K.: Optimum Relationship for the Dimensions of Thrust Bearing Pads. Russ. Eng. J., vol. 54, no. 3, Mar. 1974, pp. 9-12.

9. Tieu, A. K.: A Numerical Simulation of Finite-Width Thrust Bearings, Taking into Account Viscosity Variation with Temperature and Pressure. J. Mech. Eng. Sci., vol. 17, no. 1, Feb. 1975, pp. 1-10.

10. Sternlicht, B.; Reid, J. C., Jr.; and Arwas, E. B.: Performance of Elastic, Centrally Pivoted Sector, Thrust Bearing Pads - Part I. J. Basic Eng., Trans. ASME, ser. D, vol. 83, no. 2, pp. 169-178.

11. Sternlicht, B.; Carter, G. K.; and Arwas, E. B.: Adiabatic Analysis of Elastic, Centrally Pivoted, Sector, Thrust-Bearing Pads. J. Appl. Mech., Trans. ASME, ser. E, no. 2, June 1961, pp. 179-187.

12. Floberg, L.: On the Optimum Design of Sector-Shaped Tilting Pad Thrust Bearings. Acta Polytech. Scand. Mech. Eng. Ser., 45, 1969.

13. Etsion, Izhak· Analysis of the Gas-Lubricated, Flat-Sector-Pad Thrust Bearing. NASA TN D-8220, 1976.

14. Presler, Alden F.; and Etsion, Izhak: Computer Program for Flat Sector Thrust Bearing Performance. NASA TM X-73595, 1977.

TABLE I. - COMPARISON BETWEEN UNIT LOAD OF FLAT SECTOR-SHAPED PADS AND THEIR CORRESPONDING MICHELL BEARING PADS

Clearance ratio, h_1/h_2	Radius ratio, r_i/r_o, 1/3; angular extent of pad, β, 80^o			Radius ratio, r_i/r_o, 2/3; angular extent of pad, β, 30^o		
	Pitch line location, θ_p/β		Michell bearing approximation	Pitch line location, θ_p/β		Michell bearing approximation
	0.5	1		0.5	1	
	Unit load, $(W/KA)\times10^2$					
2	0.335	0.413	0.525	0.255	0.298	0.336
3	.312	.440	.548	.242	.312	.346
5	.216	.365	.456	.172	.255	.298
9	.113	.237	.305	.093	.164	.190

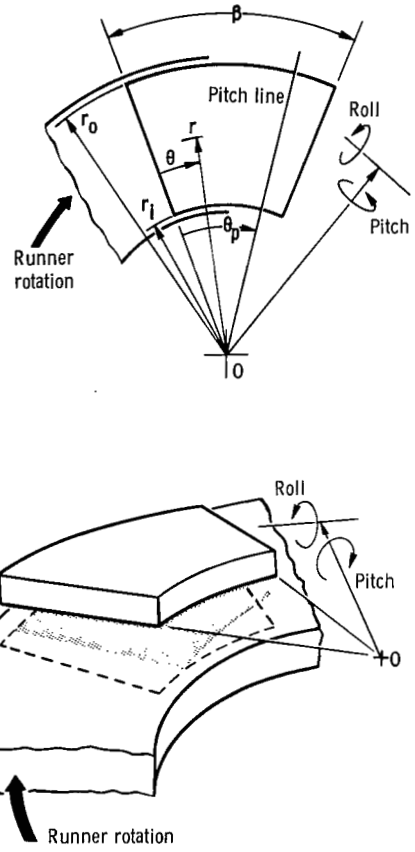

Figure 1. - Geometry of sector pad.

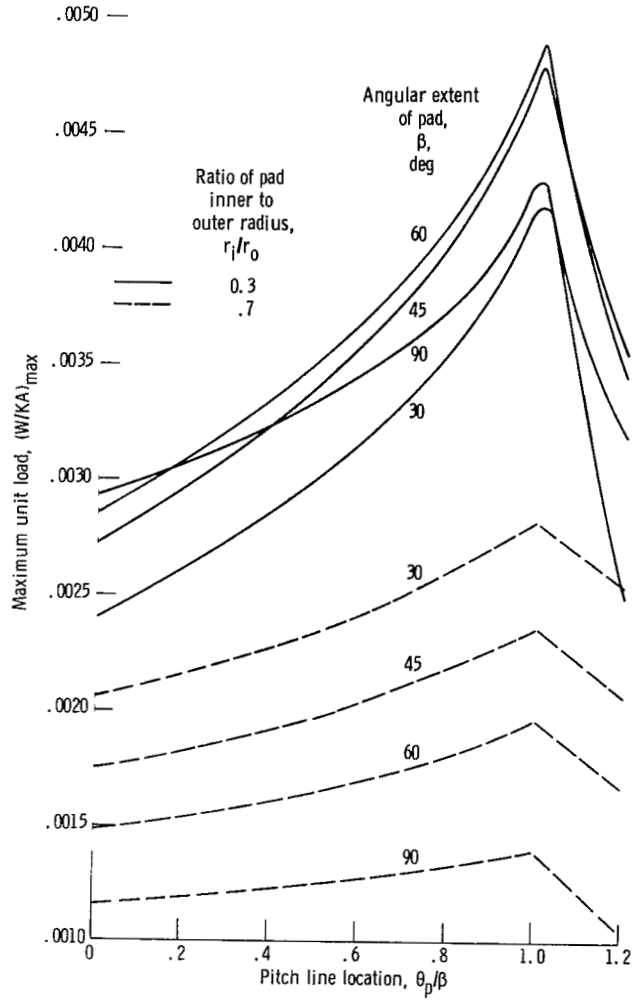

Figure 2. - Maximum available unit load as function of pivot location for various geometries.

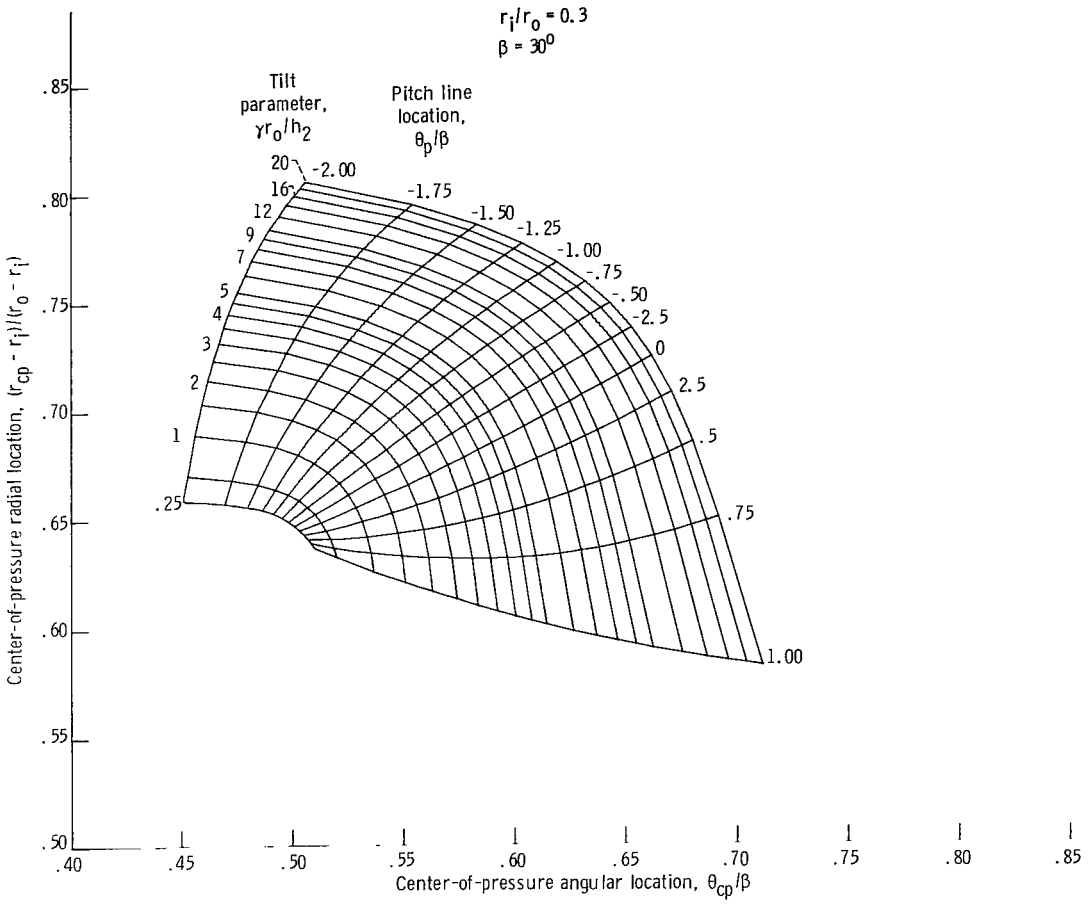

(a) Center of pressure.

Figure 3. - Design charts for flat, sector-shaped pad with ratio of inner to outer radius r_i/r_o of 0.3 and angular extent β of 30^0.

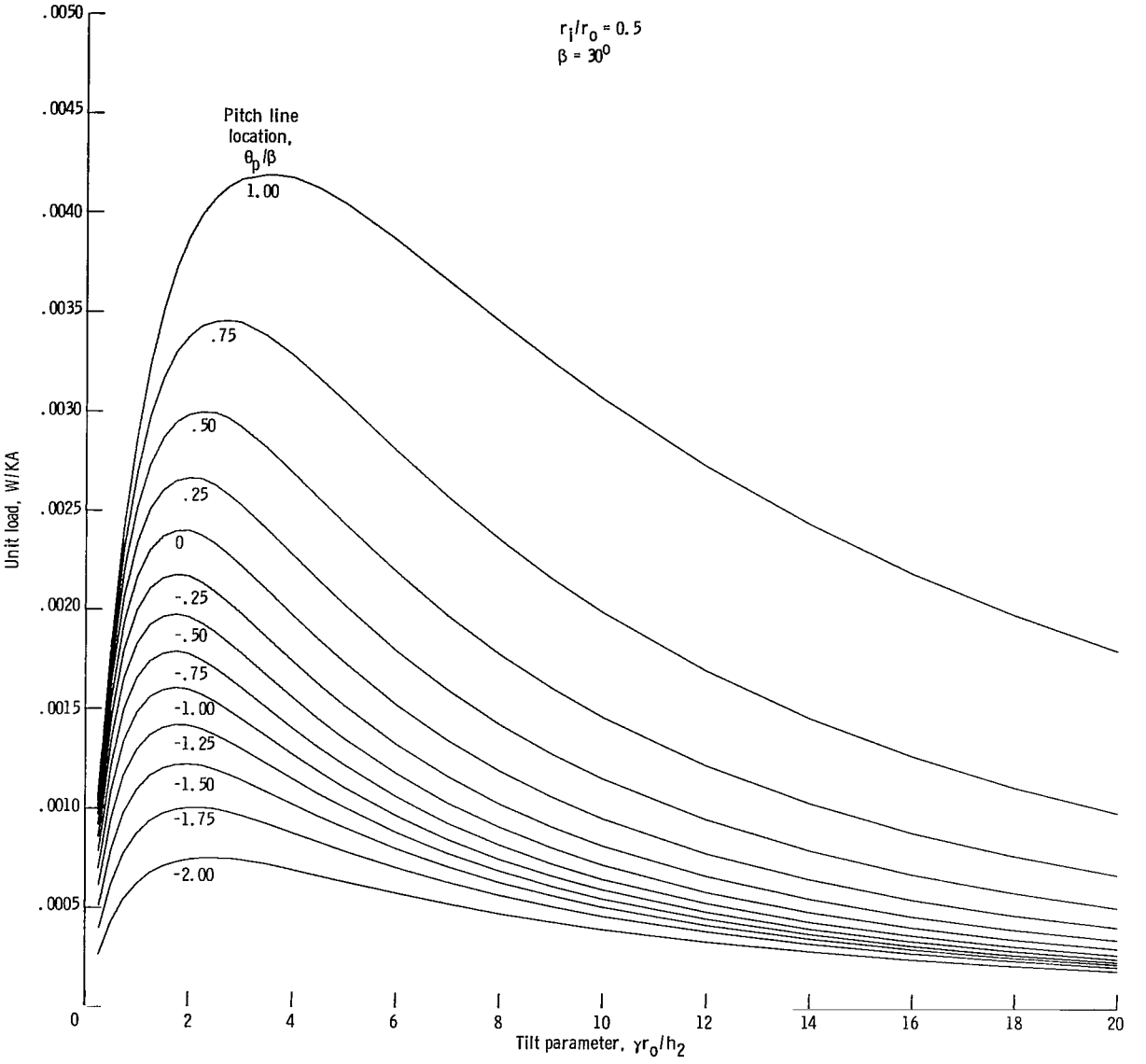

(b) Load capacity.

Figure 3. - Continued.

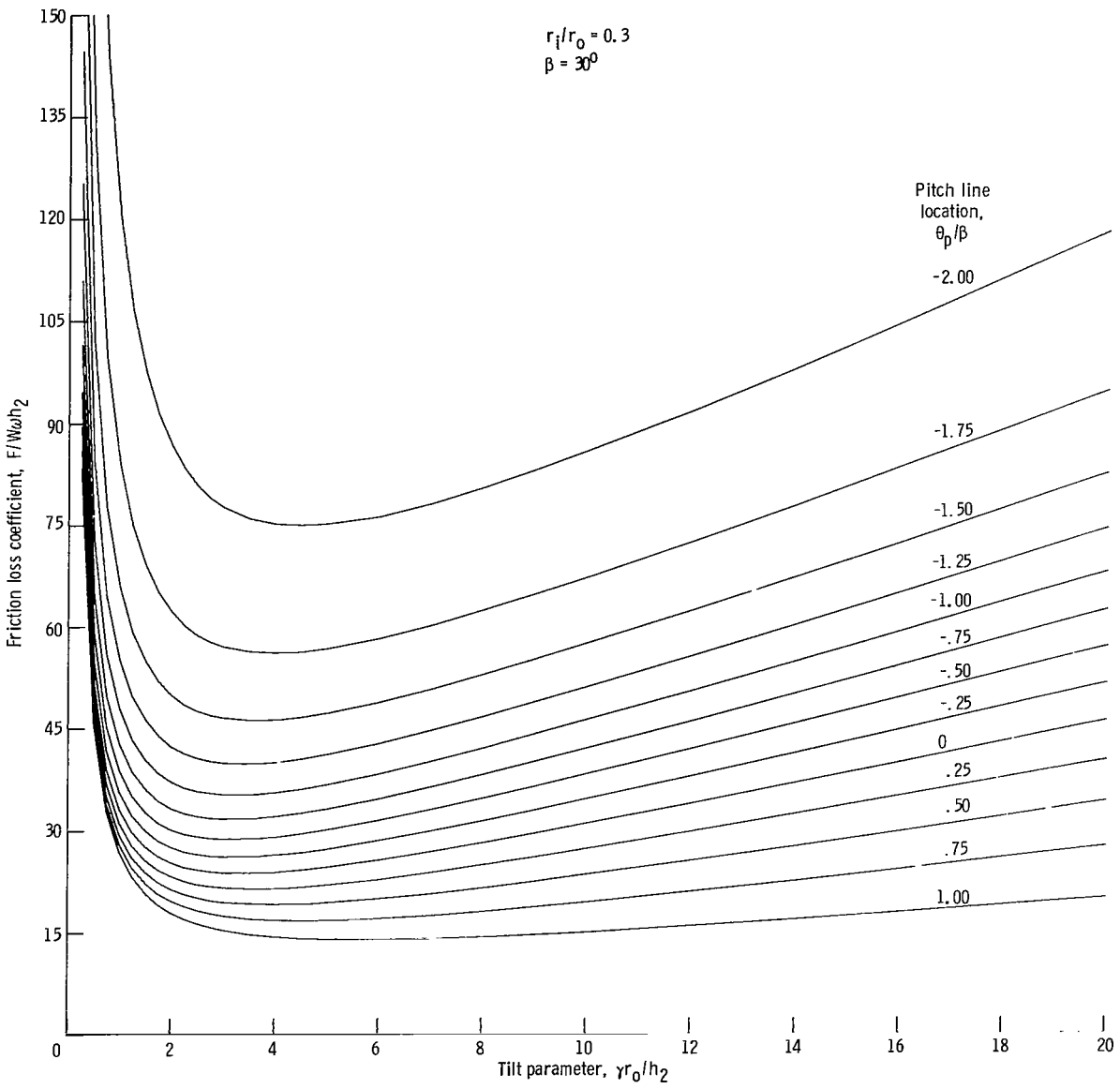

(c) Friction loss.

Figure 3. - Continued.

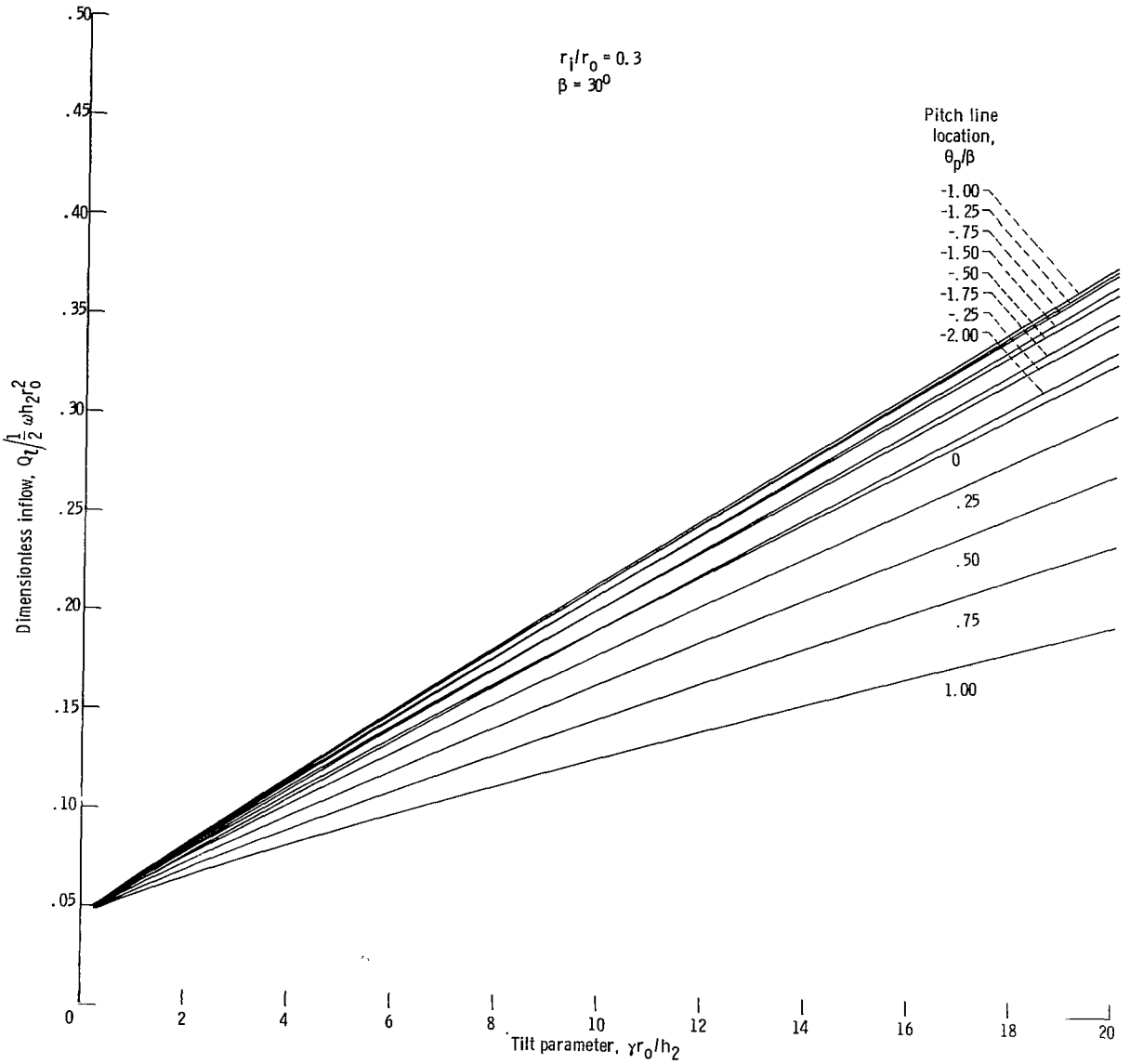

(d) Lubricant inflow.

Figure 3. - Continued.

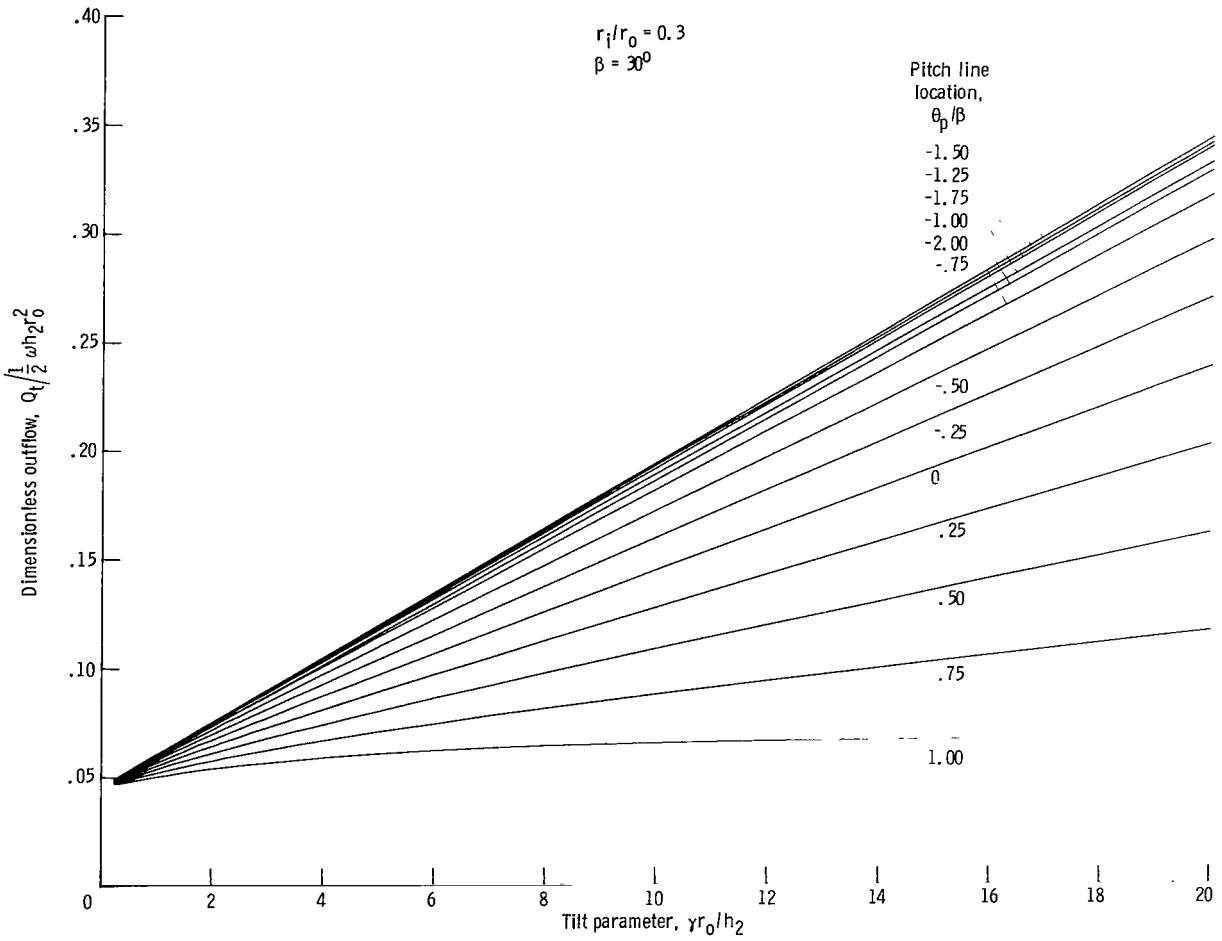

(e) Lubricant outflow at trailing edge.

Figure 3. - Concluded.

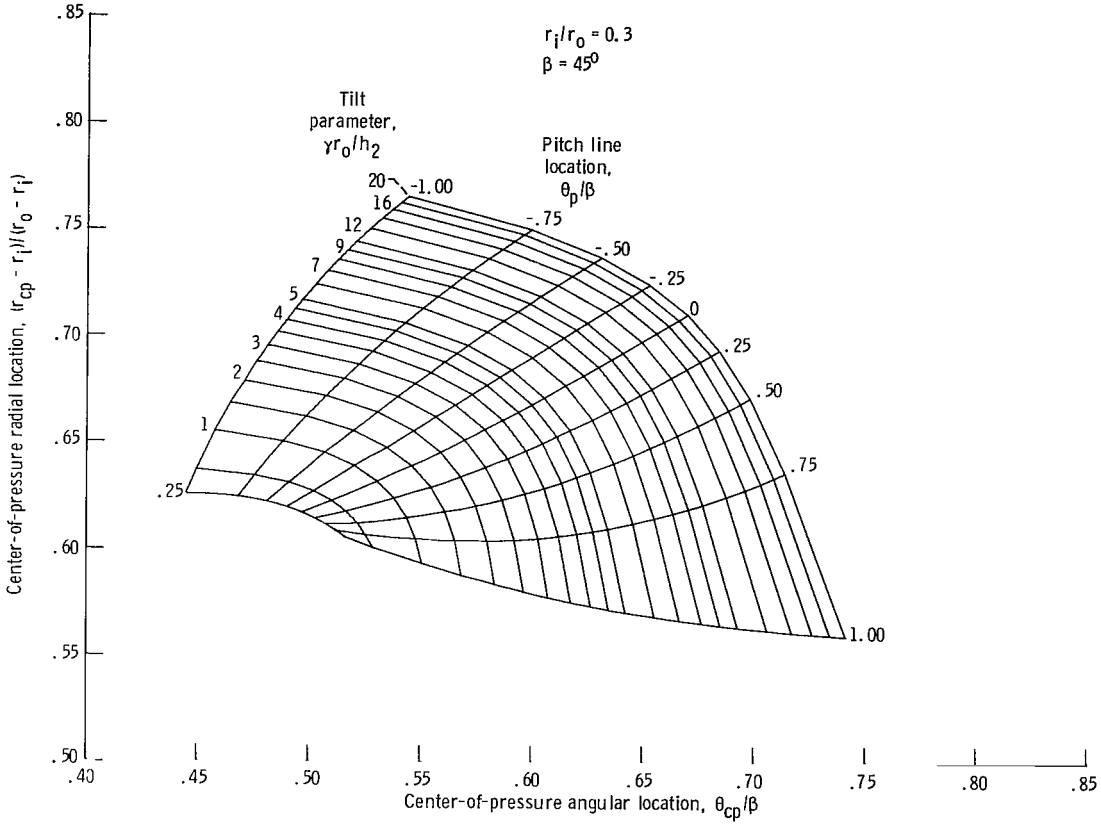

(a) Center of pressure.

Figure 4. - Design charts for flat, sector-shaped pad with ratio of inner to outer radius r_i/r_o of 0.3 and angular extent of pad β of 45^0.

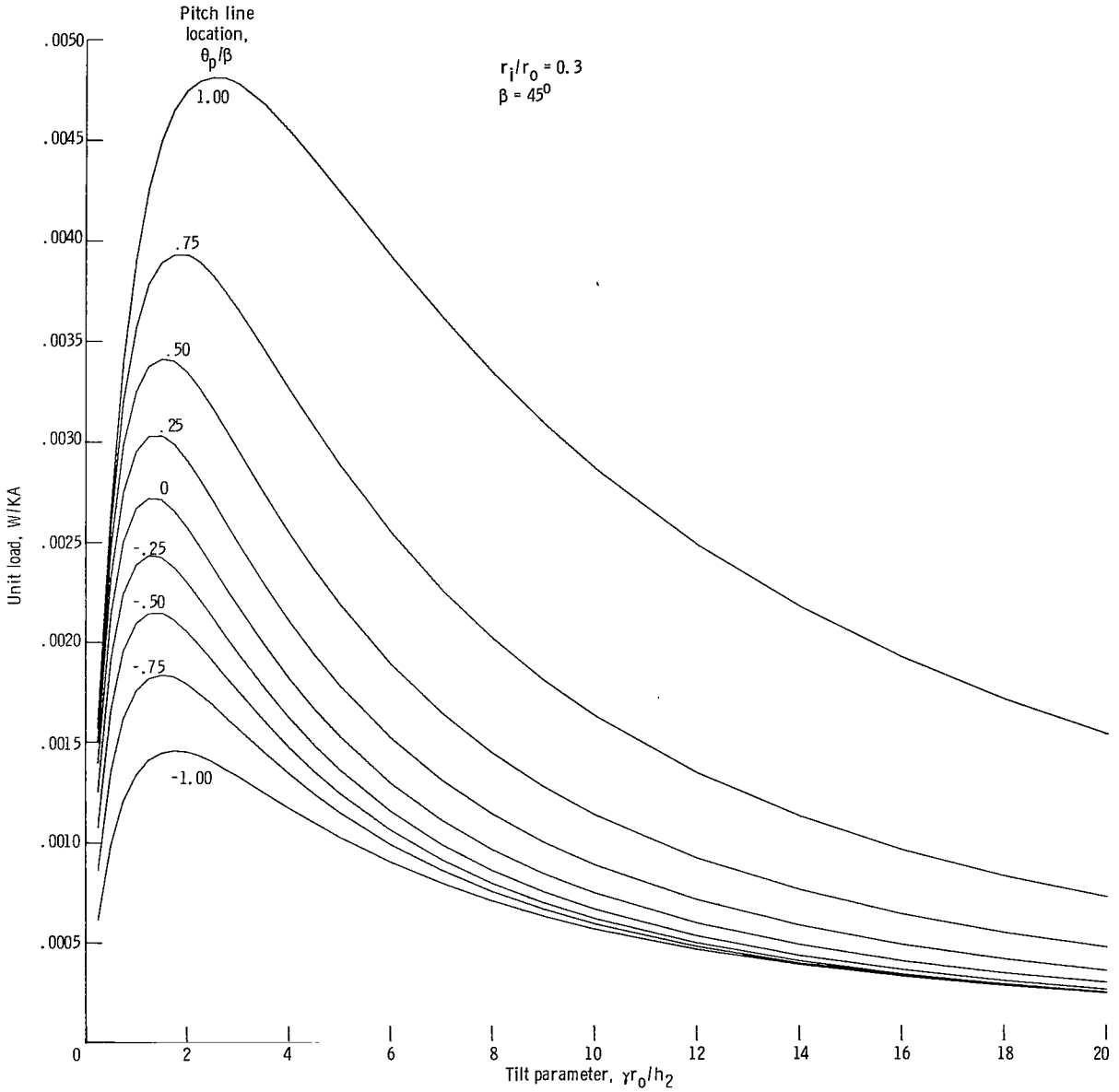

(b) Load capacity.

Figure 4. - Continued.

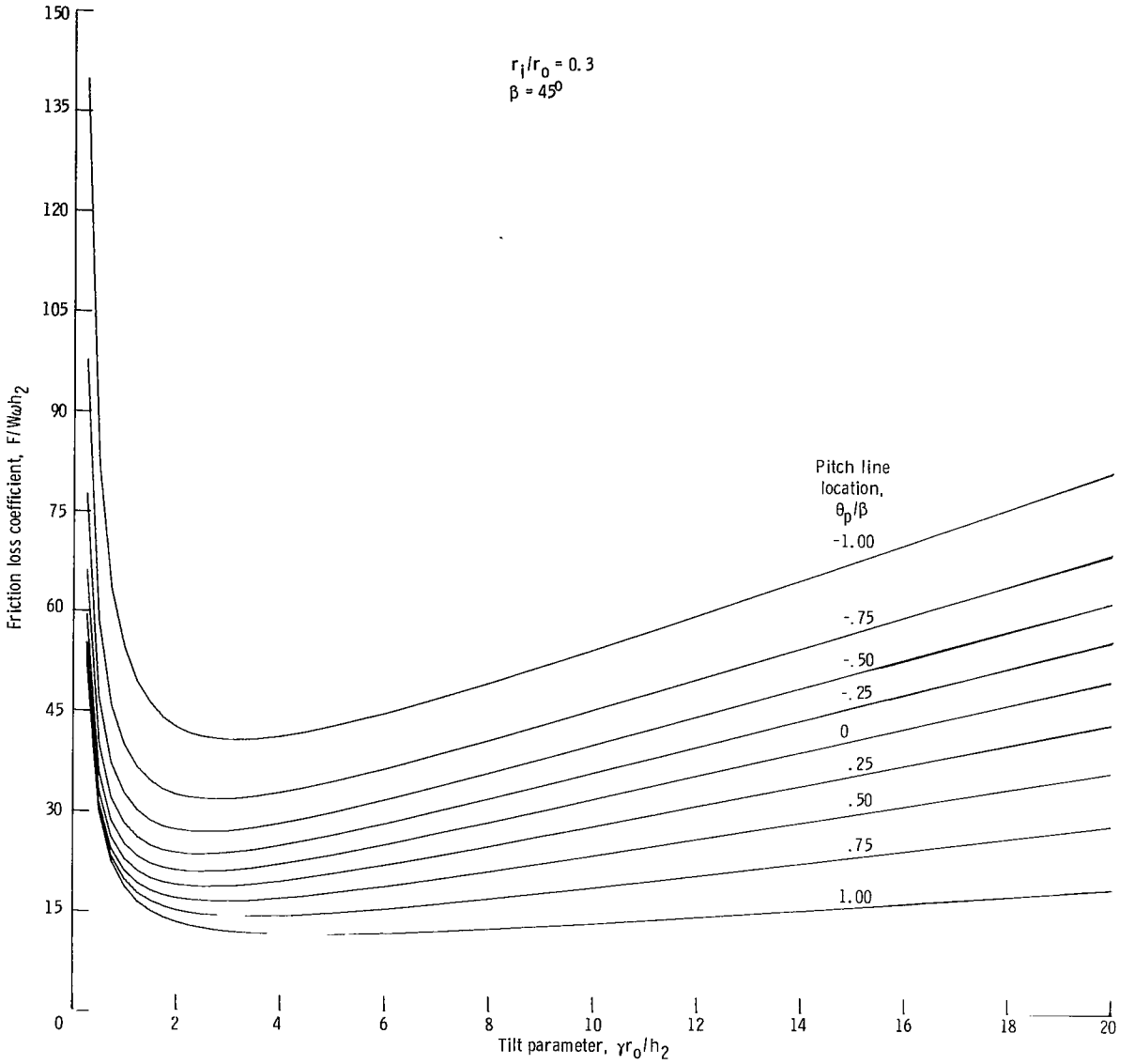

(c) Friction loss.

Figure 4. - Continued.

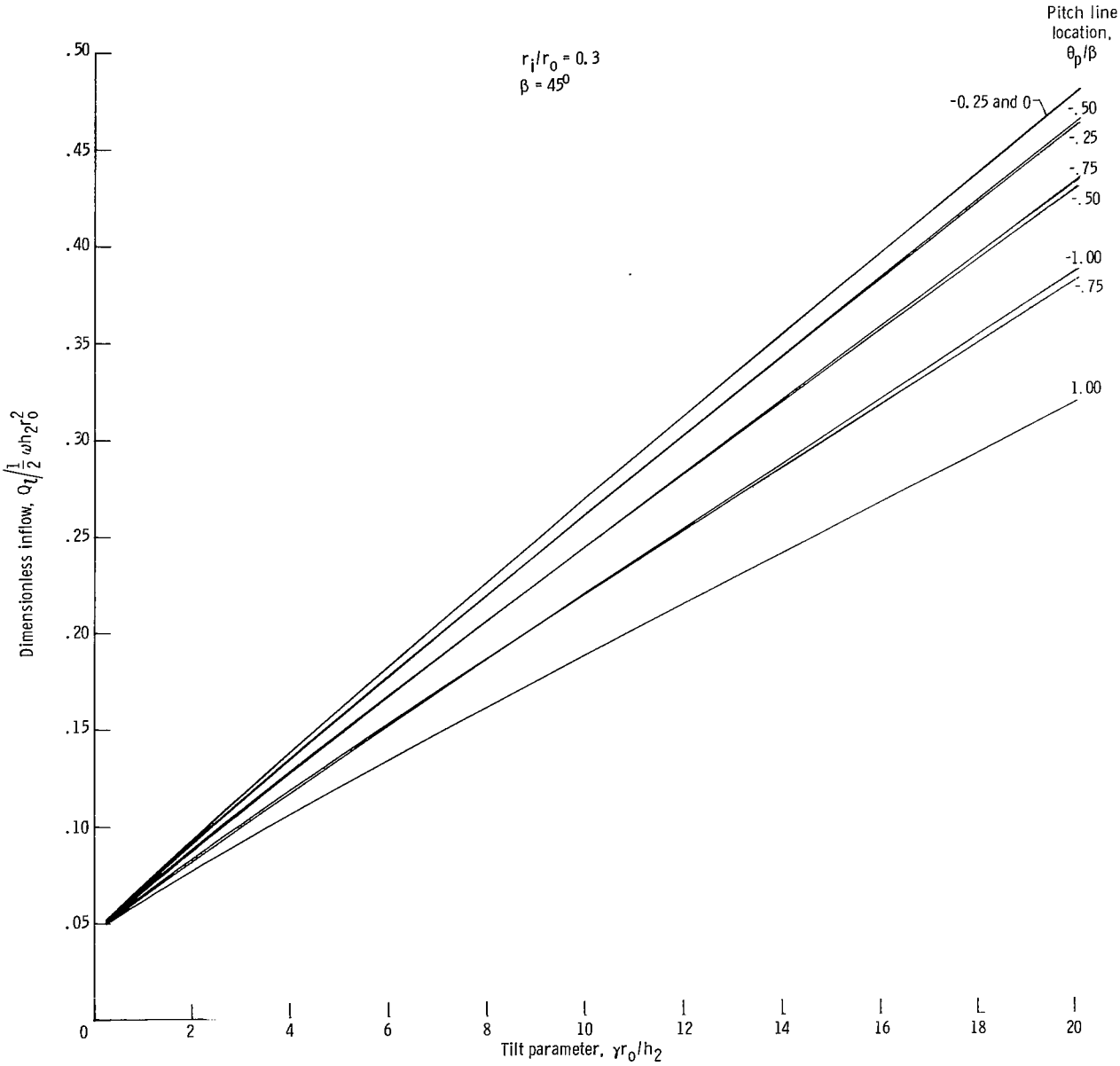

(d) Lubricant inflow.

Figure 4. - Continued.

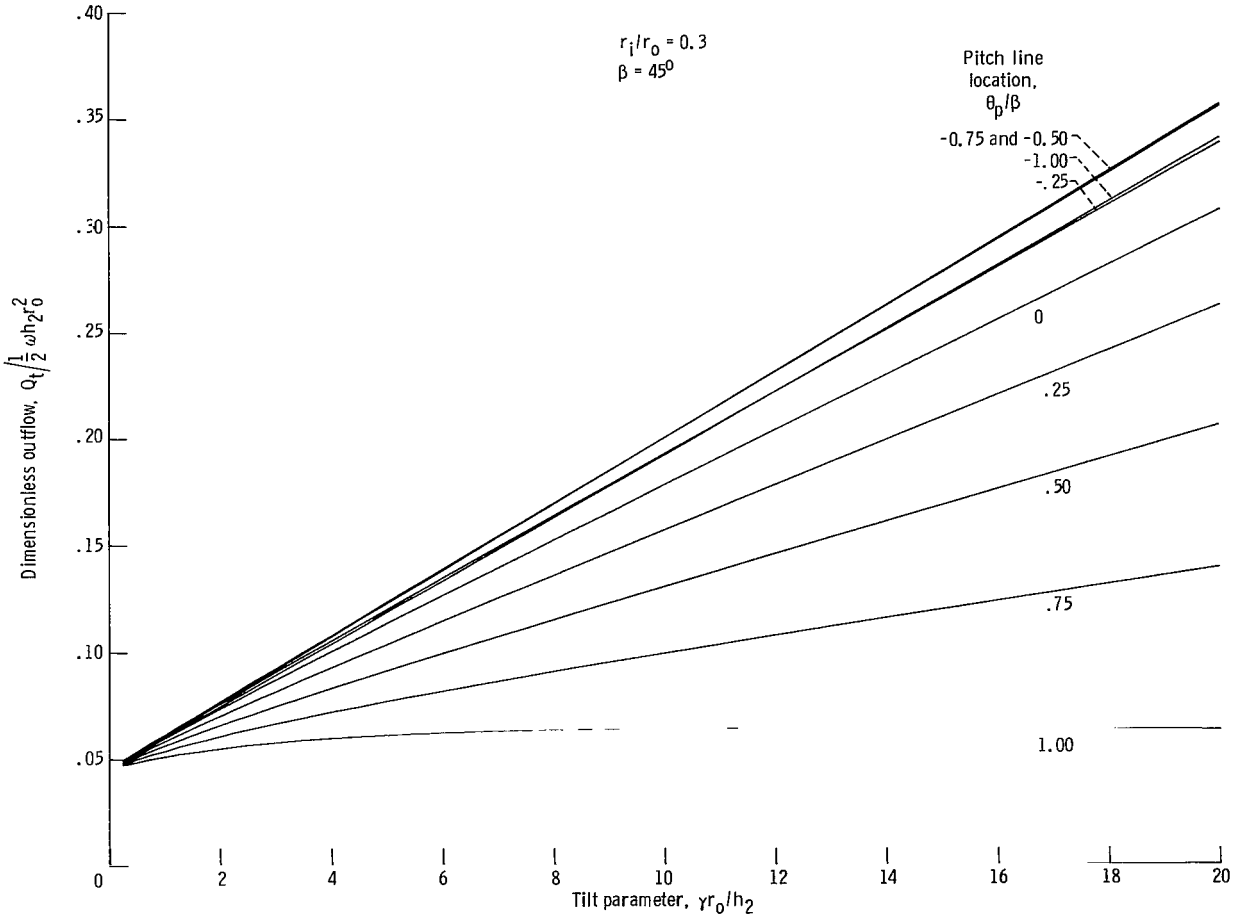

(e) Lubricant outflow at trailing edge.

Figure 4. - Concluded.

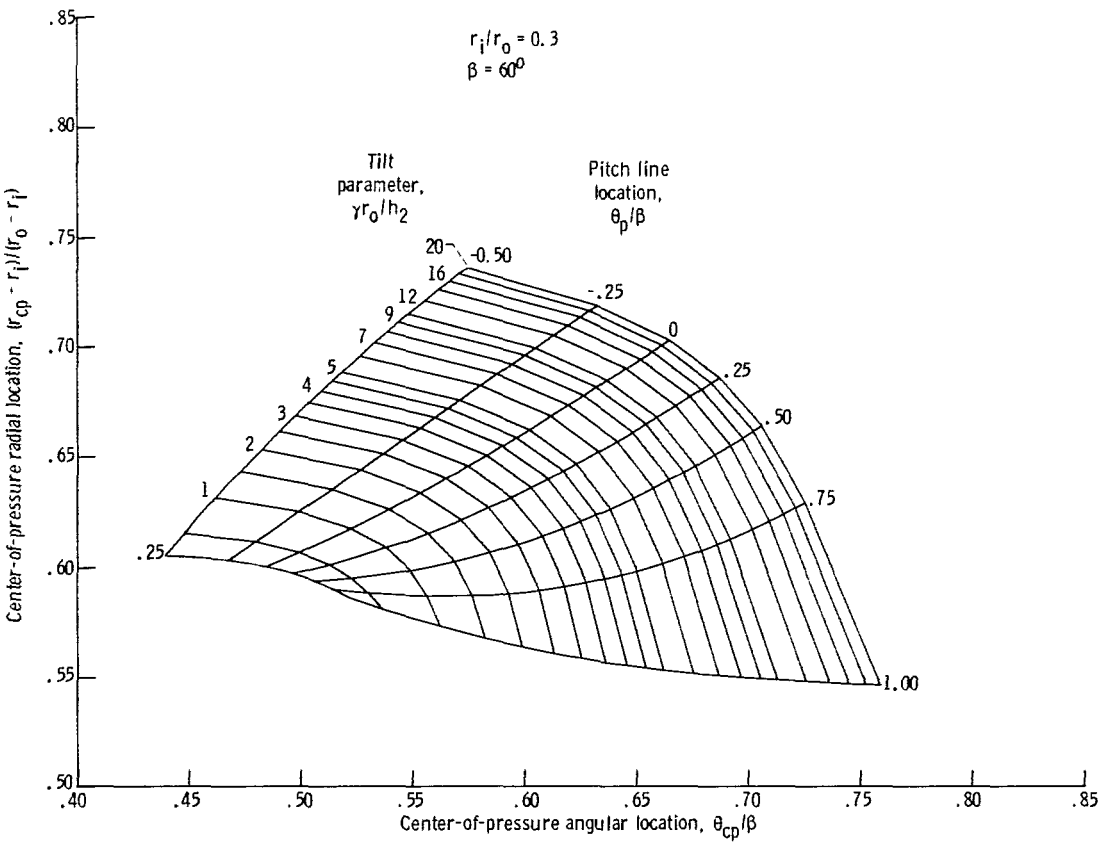

(a) Center of pressure.

Figure 5. - Design charts for flat, sector-shaped pad with ratio of inner to outer radius r_i/r_o of 0.3 and angular extent of pad β of 60^0.

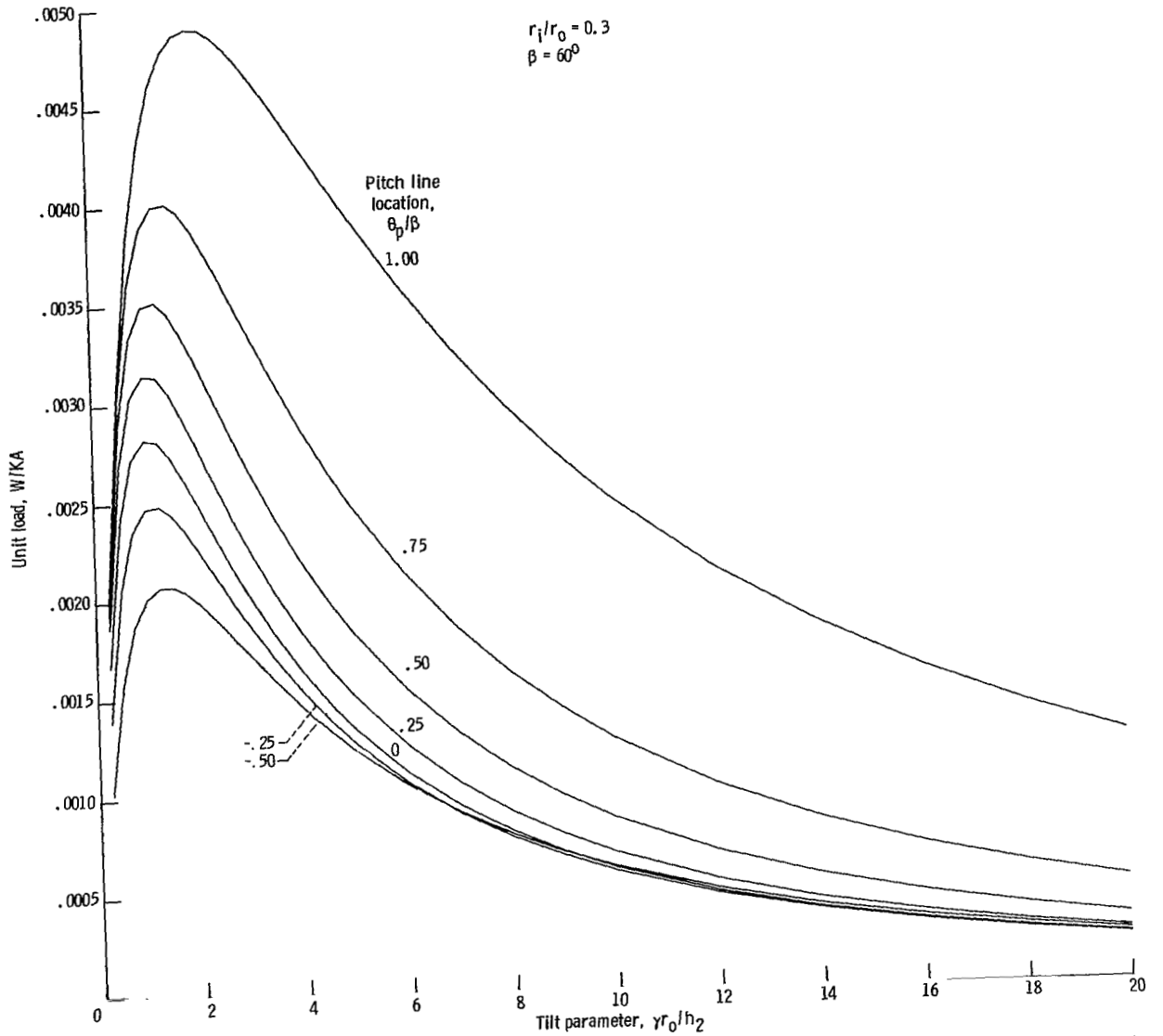

(b) Load capacity.

Figure 5. - Continued.

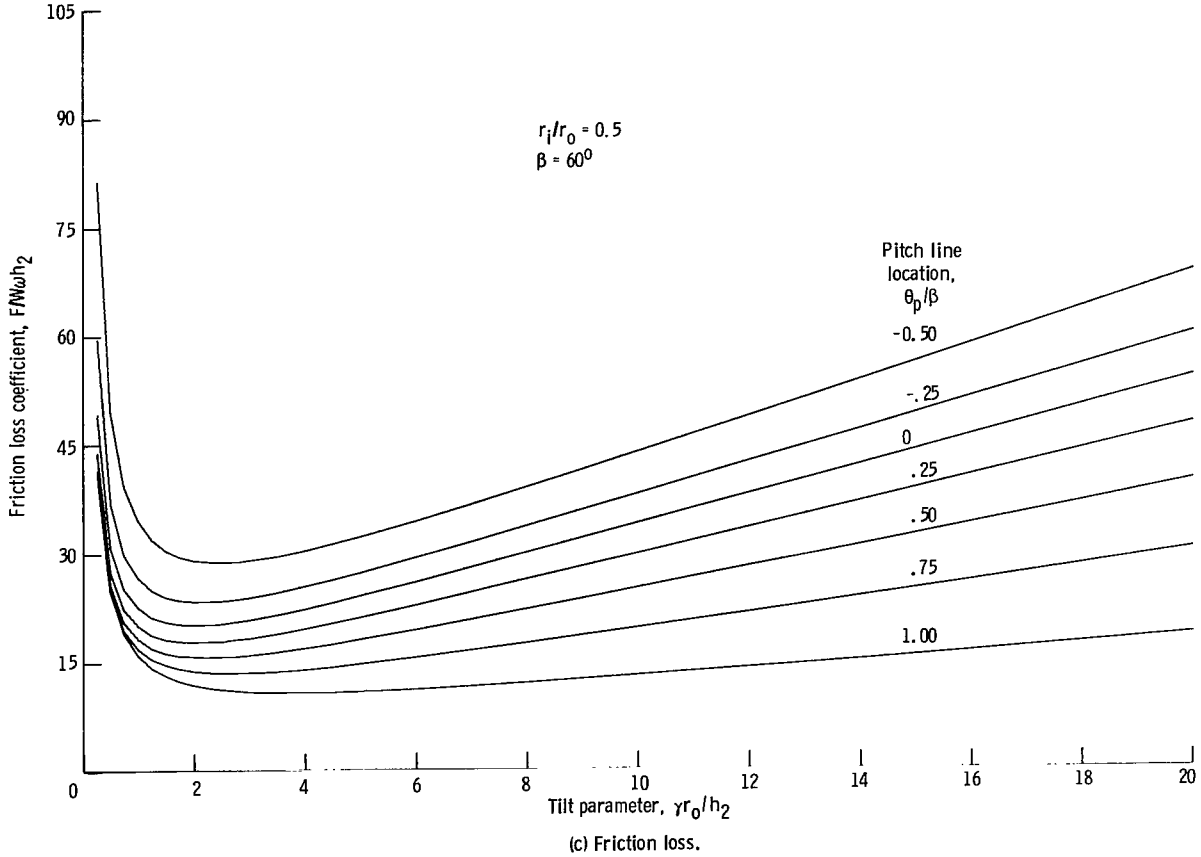

(c) Friction loss.

Figure 5. - Continued.

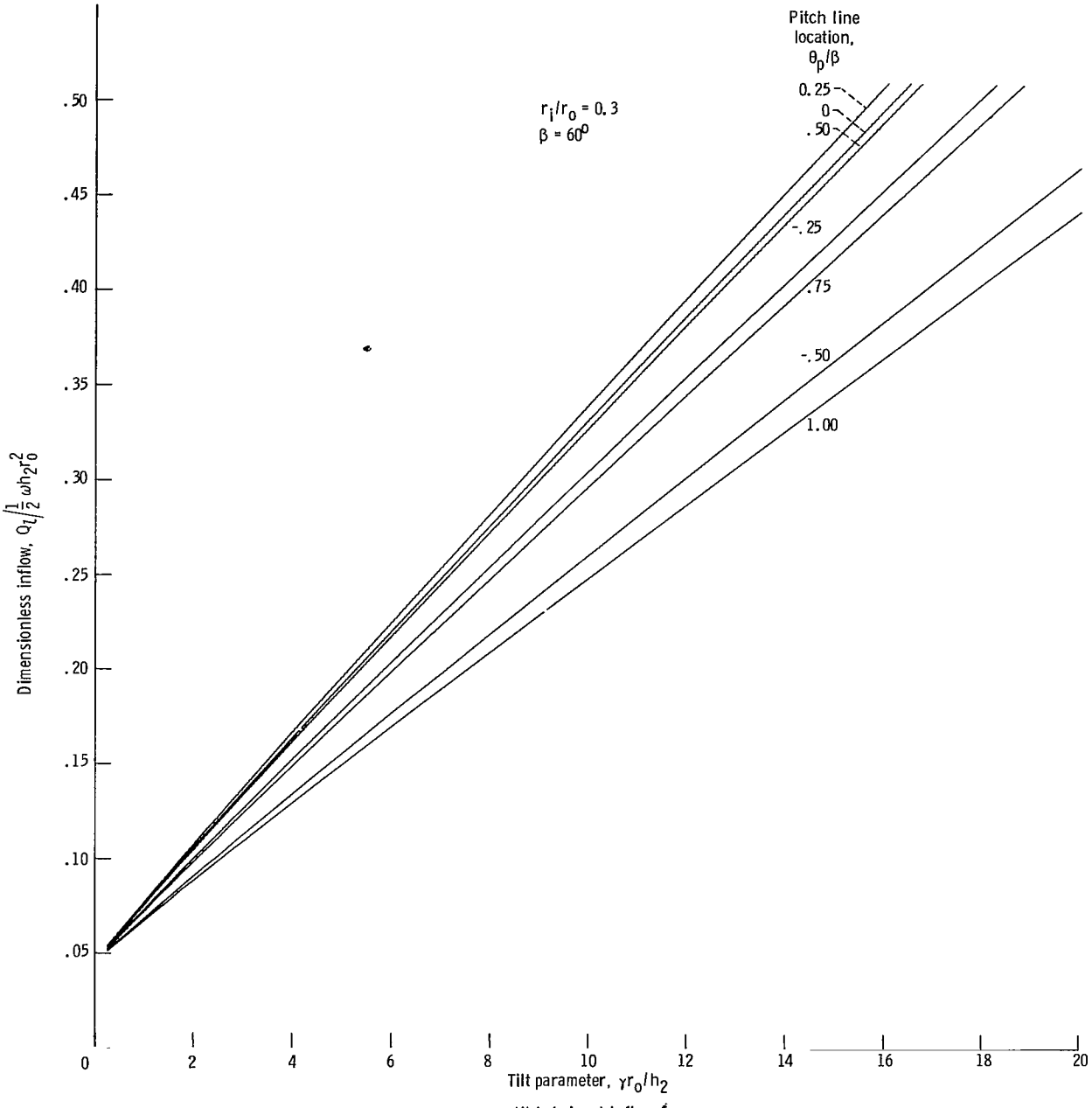

(d) Lubricant inflow.

Figure 5. - Continued.

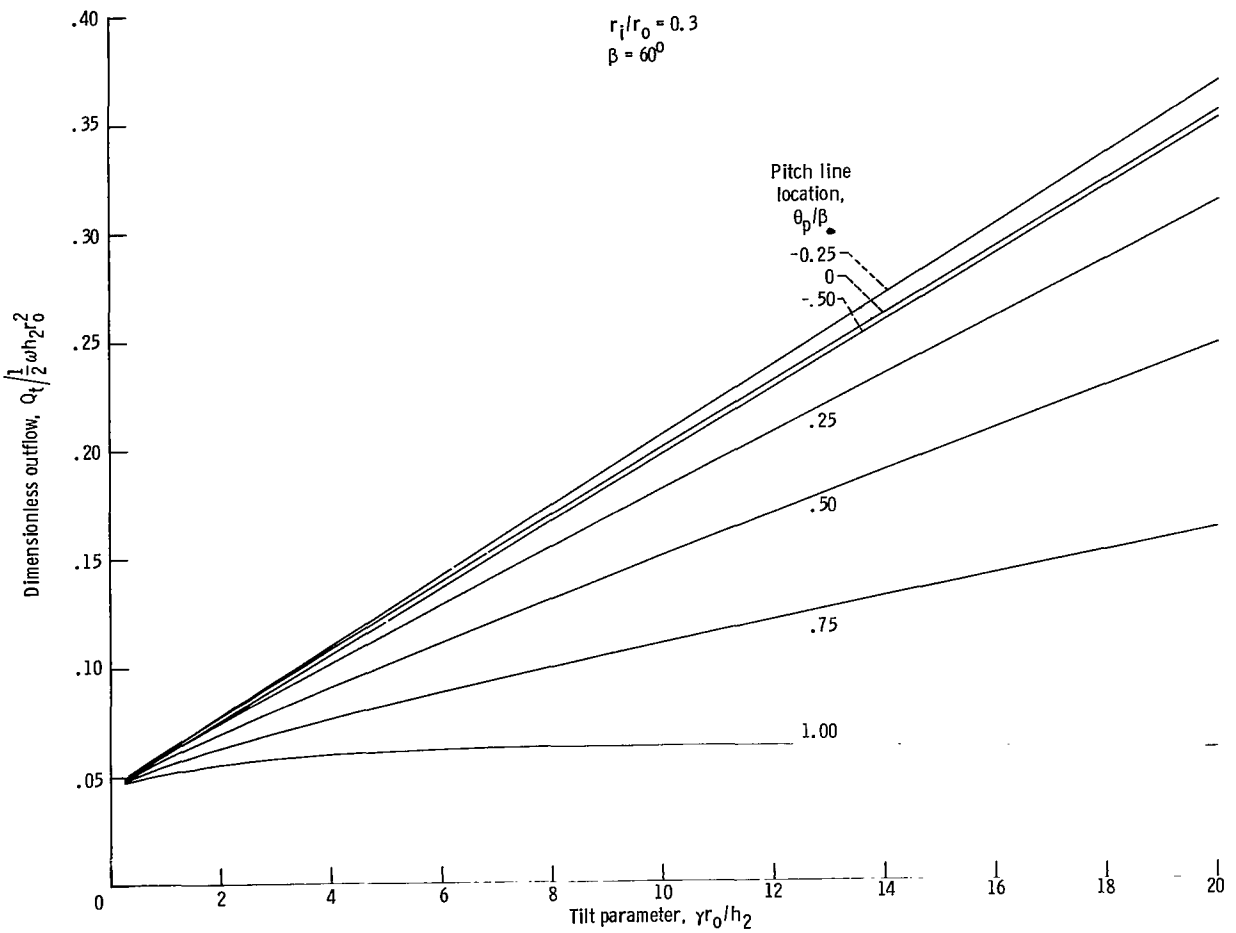

(e) Lubricant outflow at trailing edge.

Figure 5. - Concluded.

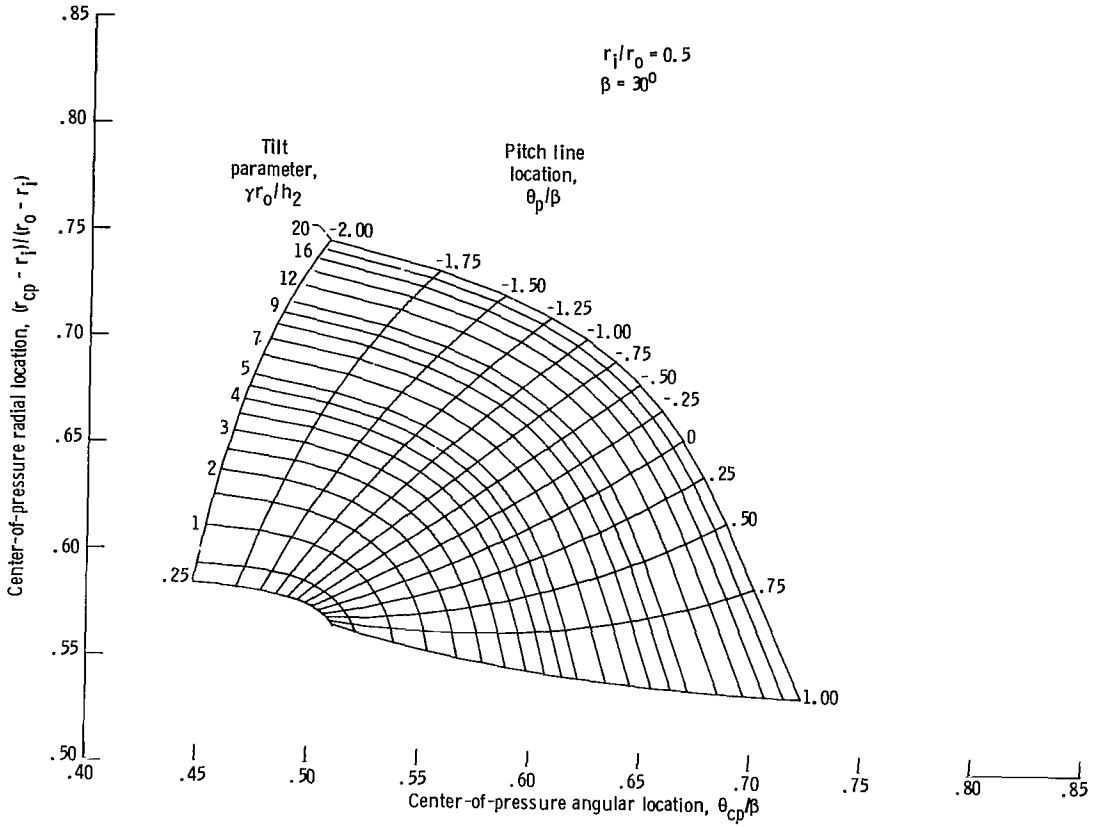

(a) Center of pressure.

Figure 6. - Design charts for flat, sector-shaped pad with ratio of inner to outer radius r_i/r_o of 0.5 and angular extent β of 30^0.

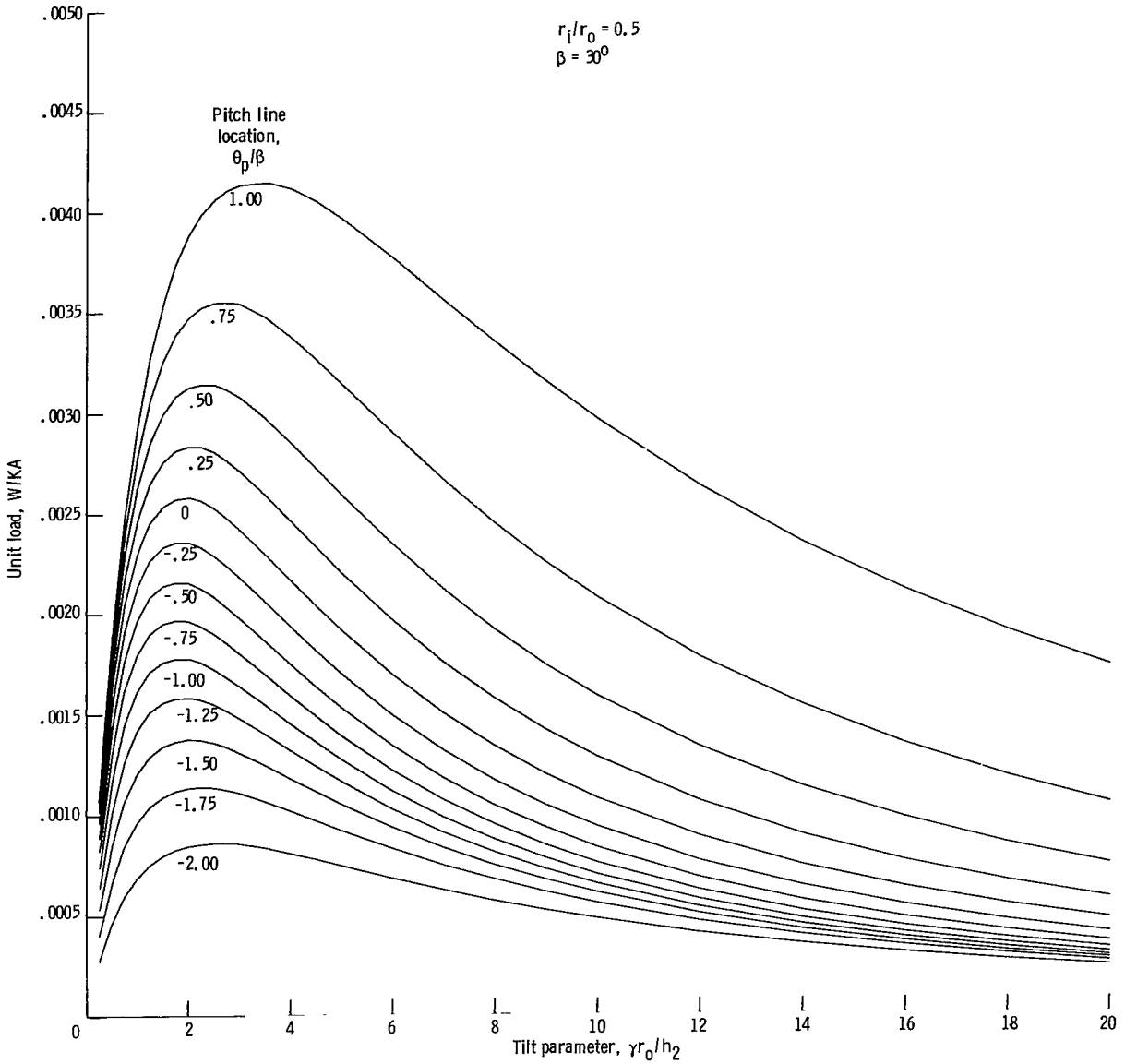

(b) Load capacity.

Figure 6. - Continued.

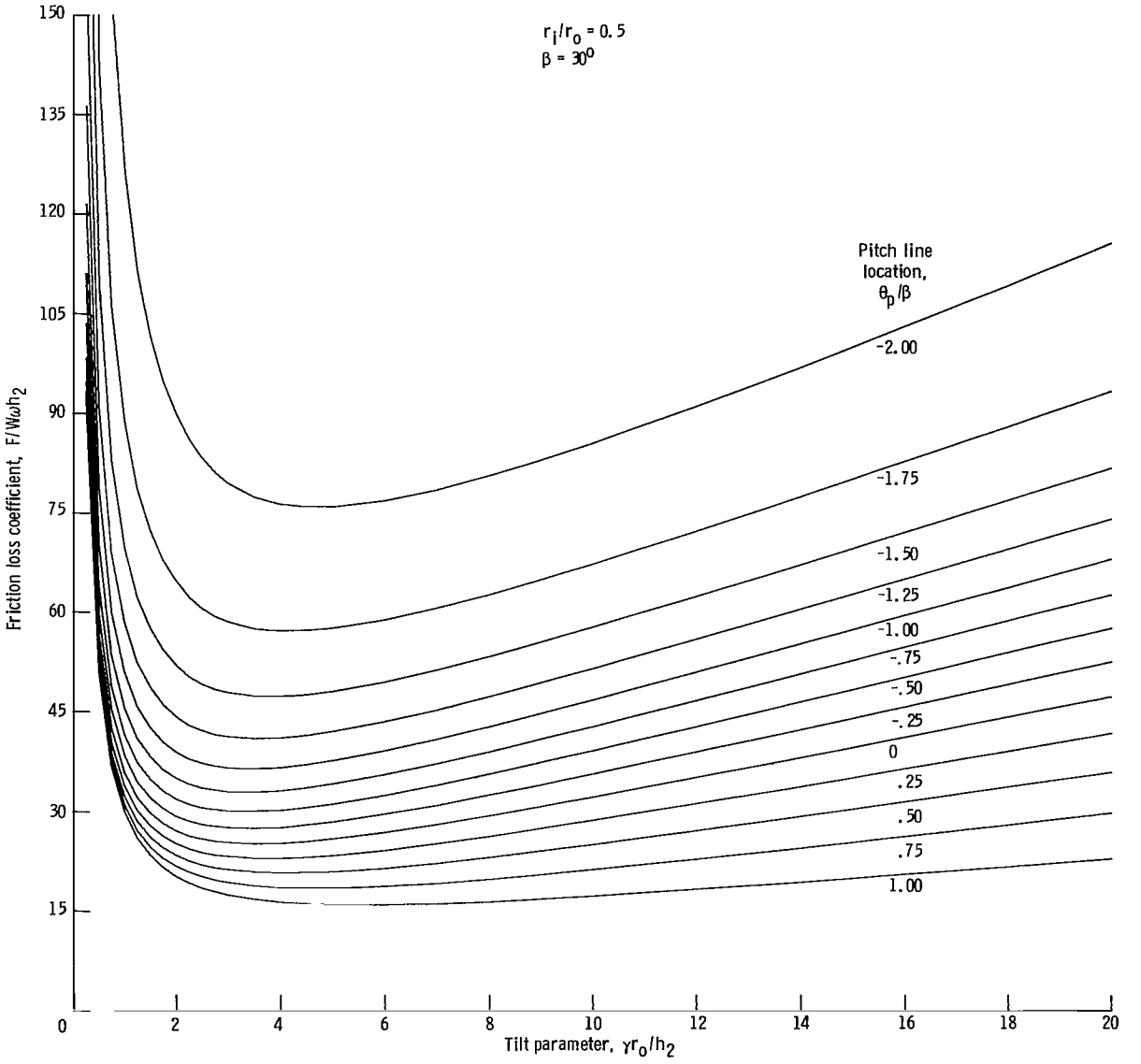

(c) Friction loss.

Figure 6. - Continued.

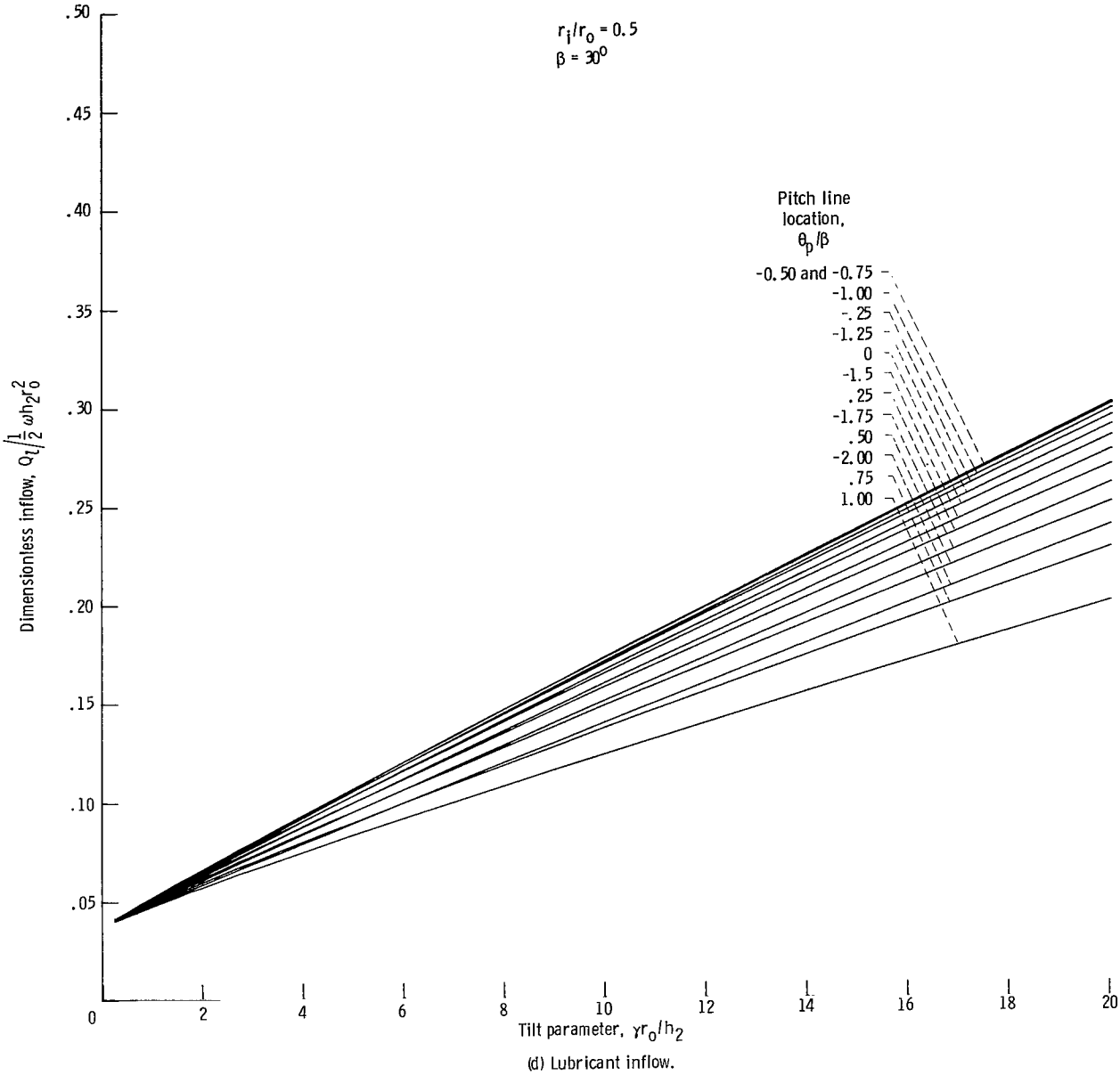

(d) Lubricant inflow.

Figure 6. - Continued.

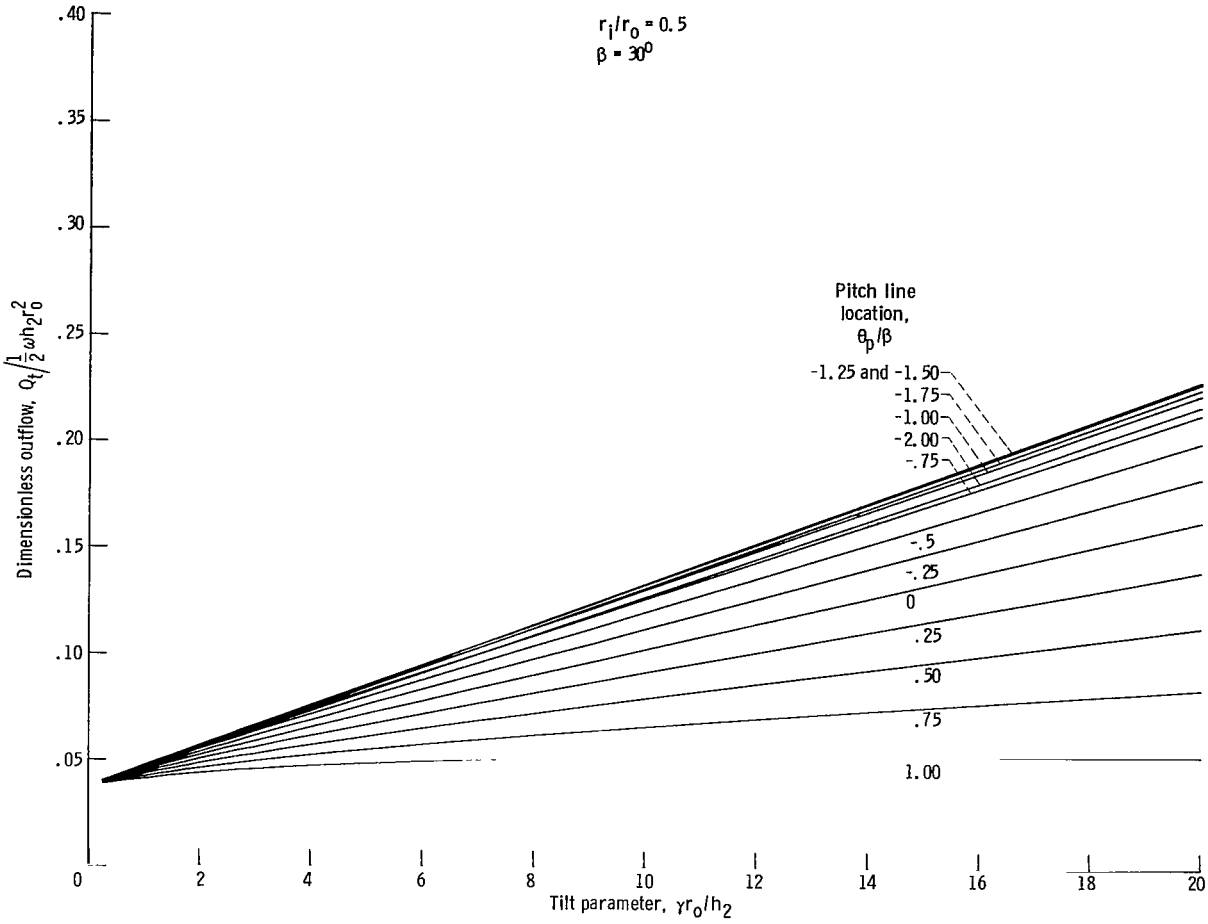

(e) Lubricant outflow at trailing edge.

Figure 6. - Concluded.

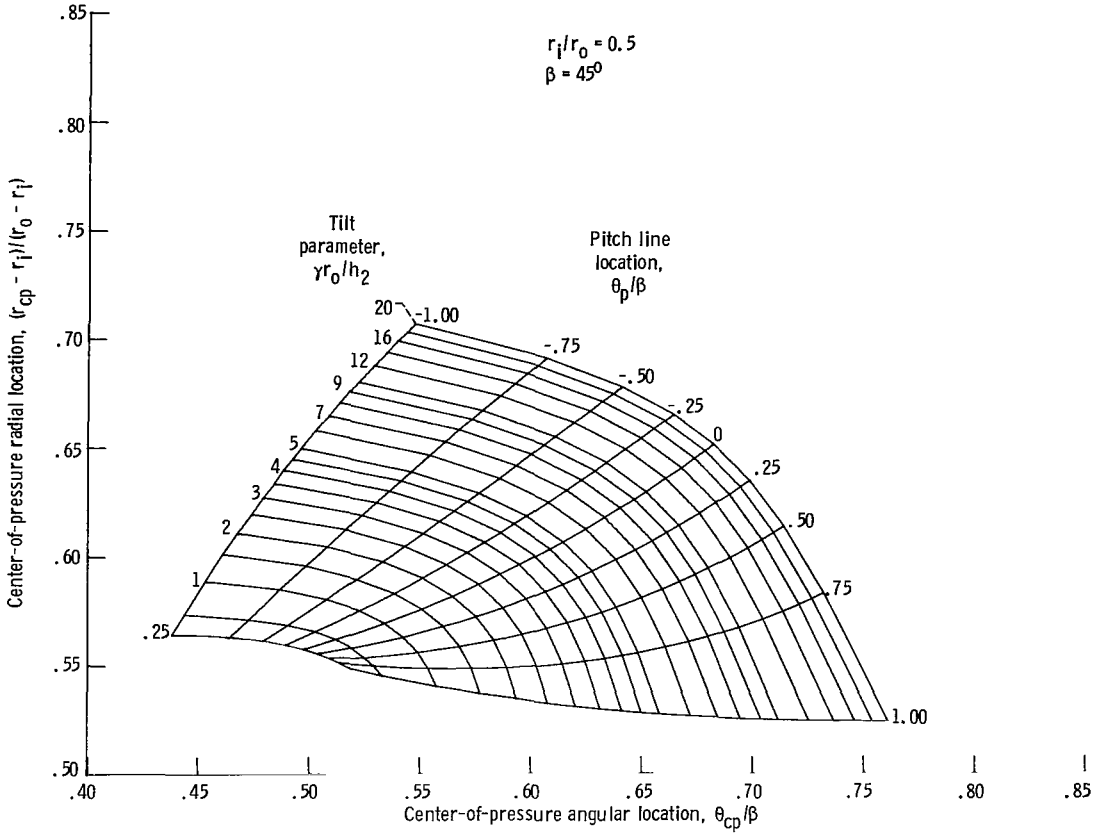

(a) Center of pressure.

Figure 7. - Design charts for flat, sector-shaped pad with ratio of inner to outer radius r_i/r_o of 0.5 and angular extent β of 45^0.

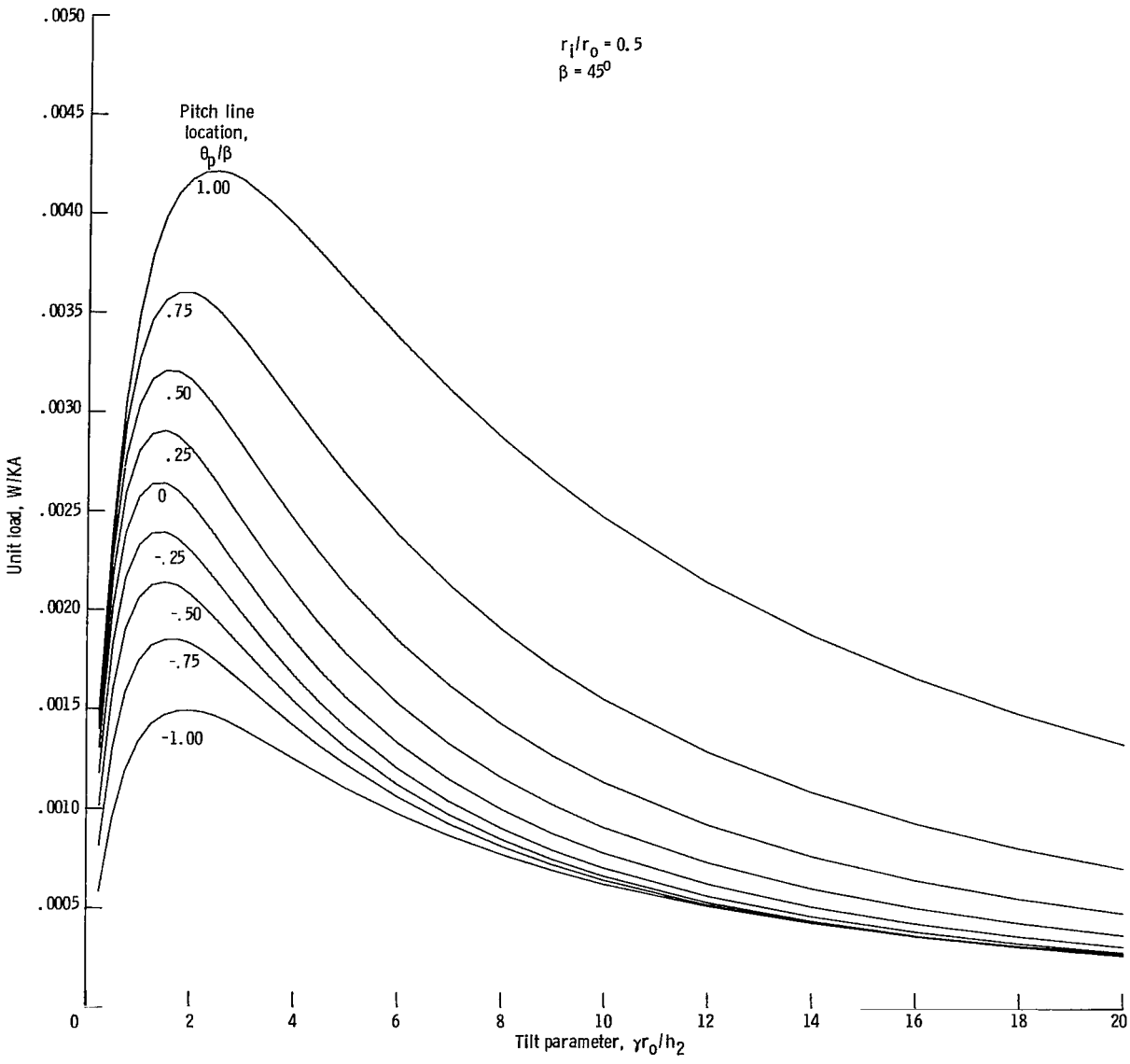

(b) Load capacity.

Figure 7. - Continued.

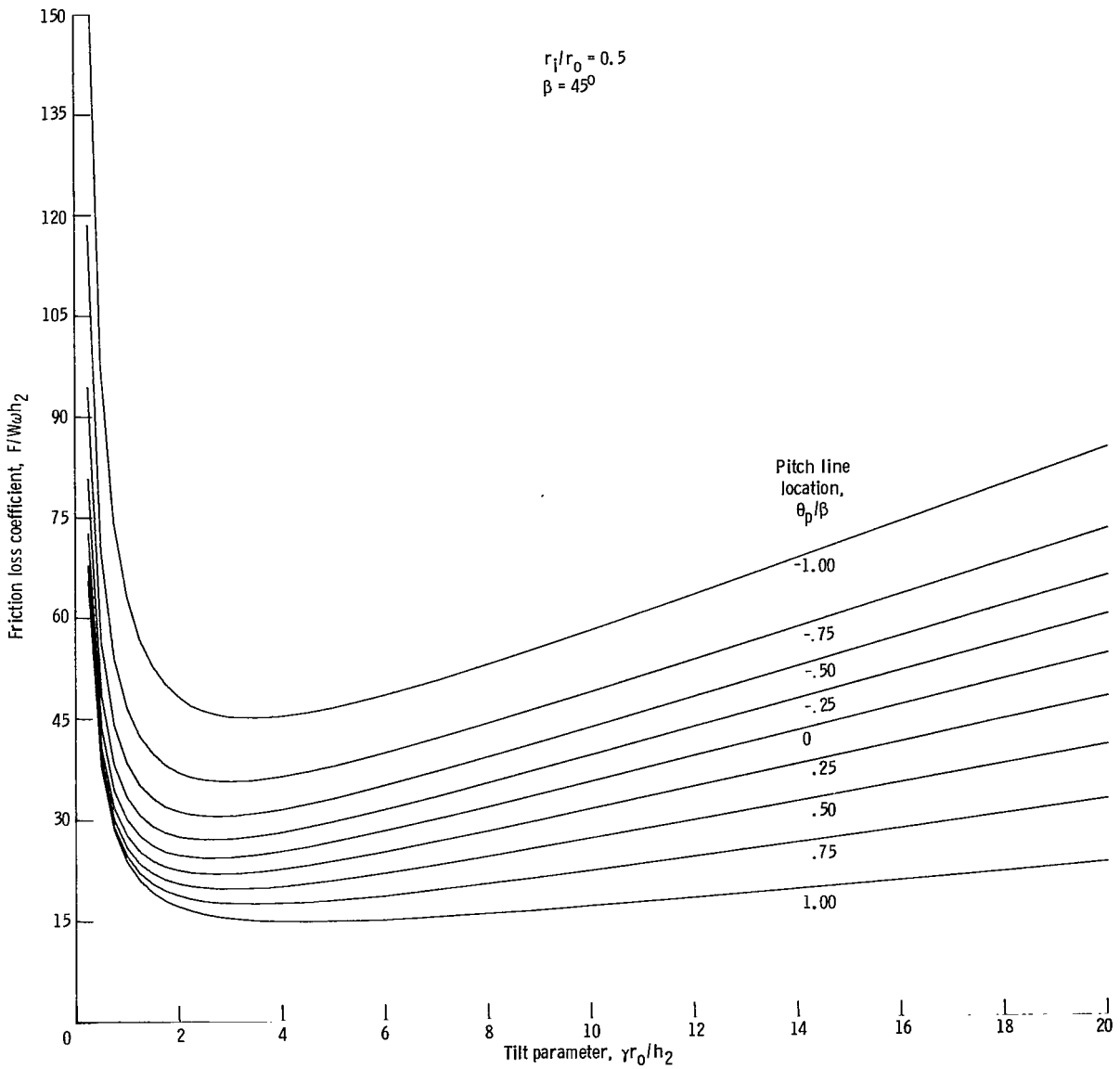

(c) Friction loss.

Figure 7. - Continued.

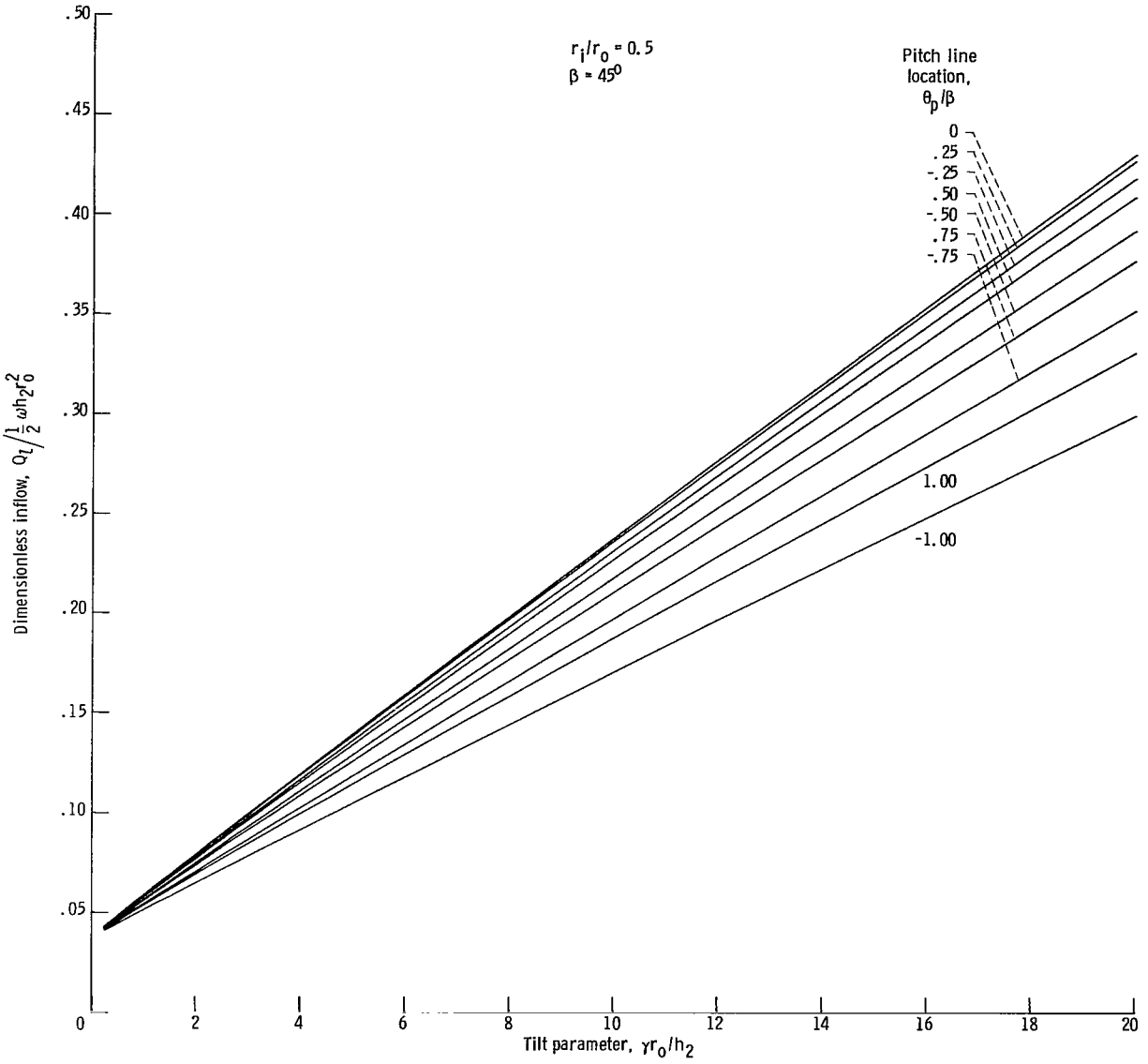

(d) Lubricant inflow.

Figure 7. - Continued.

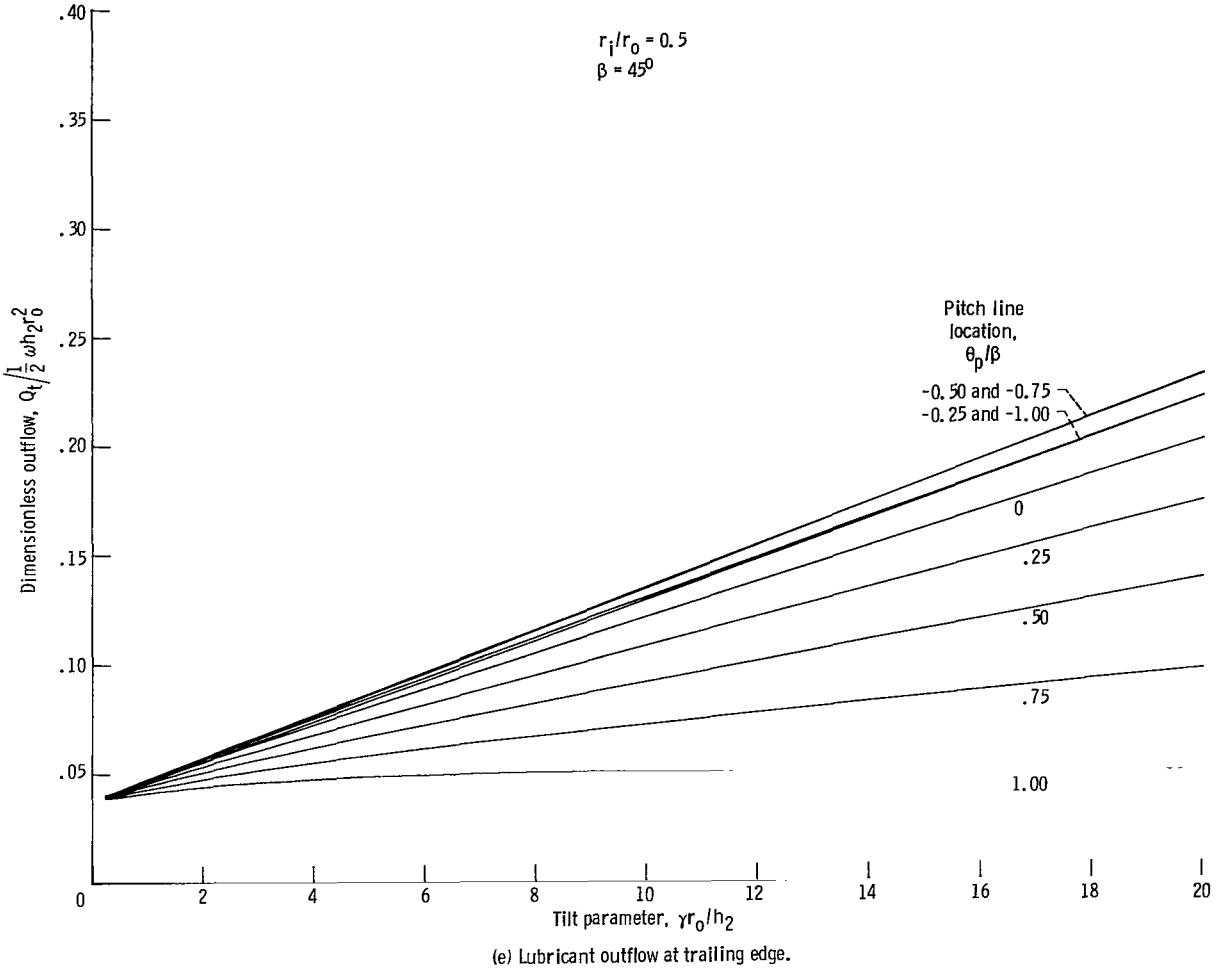

(e) Lubricant outflow at trailing edge.

Figure 7. - Concluded.

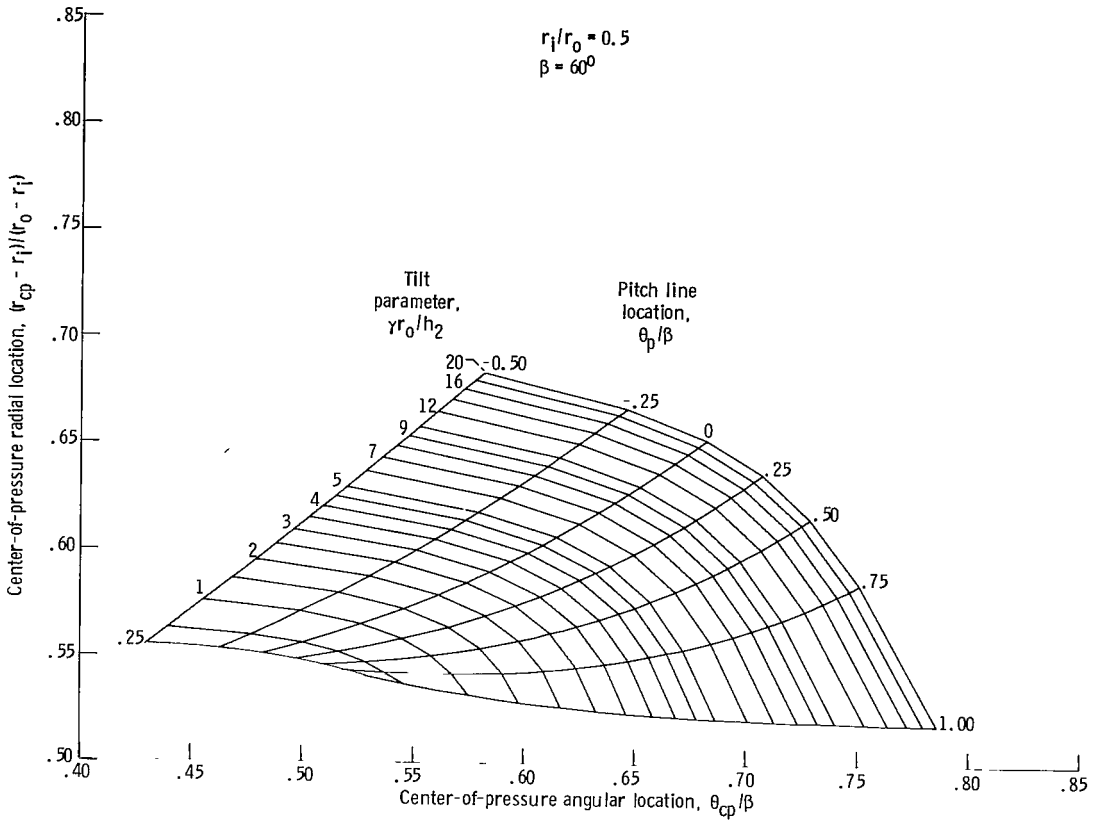

(a) Center of pressure.

Figure 8. - Design charts for flat, sector-shaped pad with ratio of inner to outer radius r_i/r_o of 0.5 and angular extent β of 60^0.

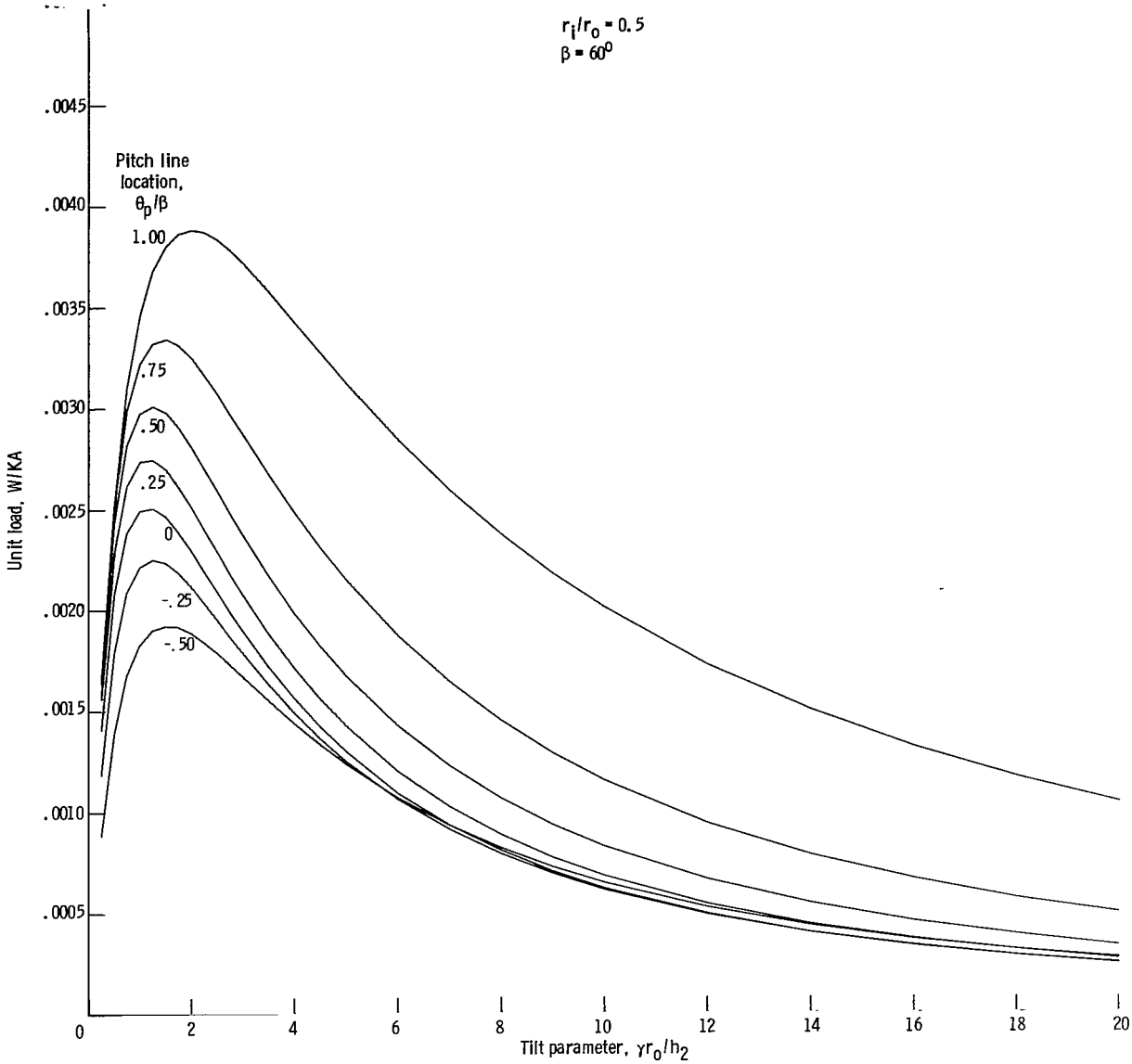

(b) Load capacity.

Figure 8. - Continued.

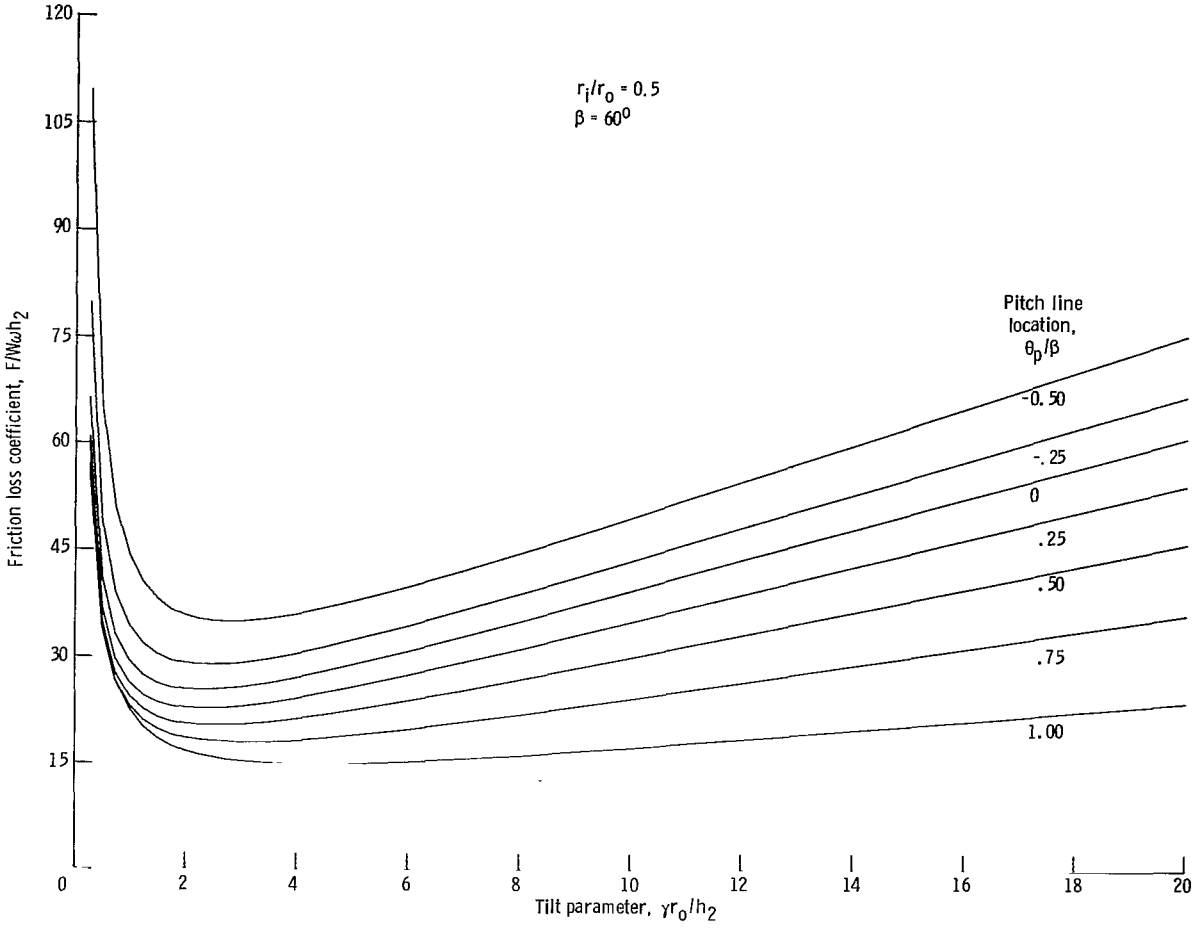

(c) Friction loss.

Figure 8. - Continued.

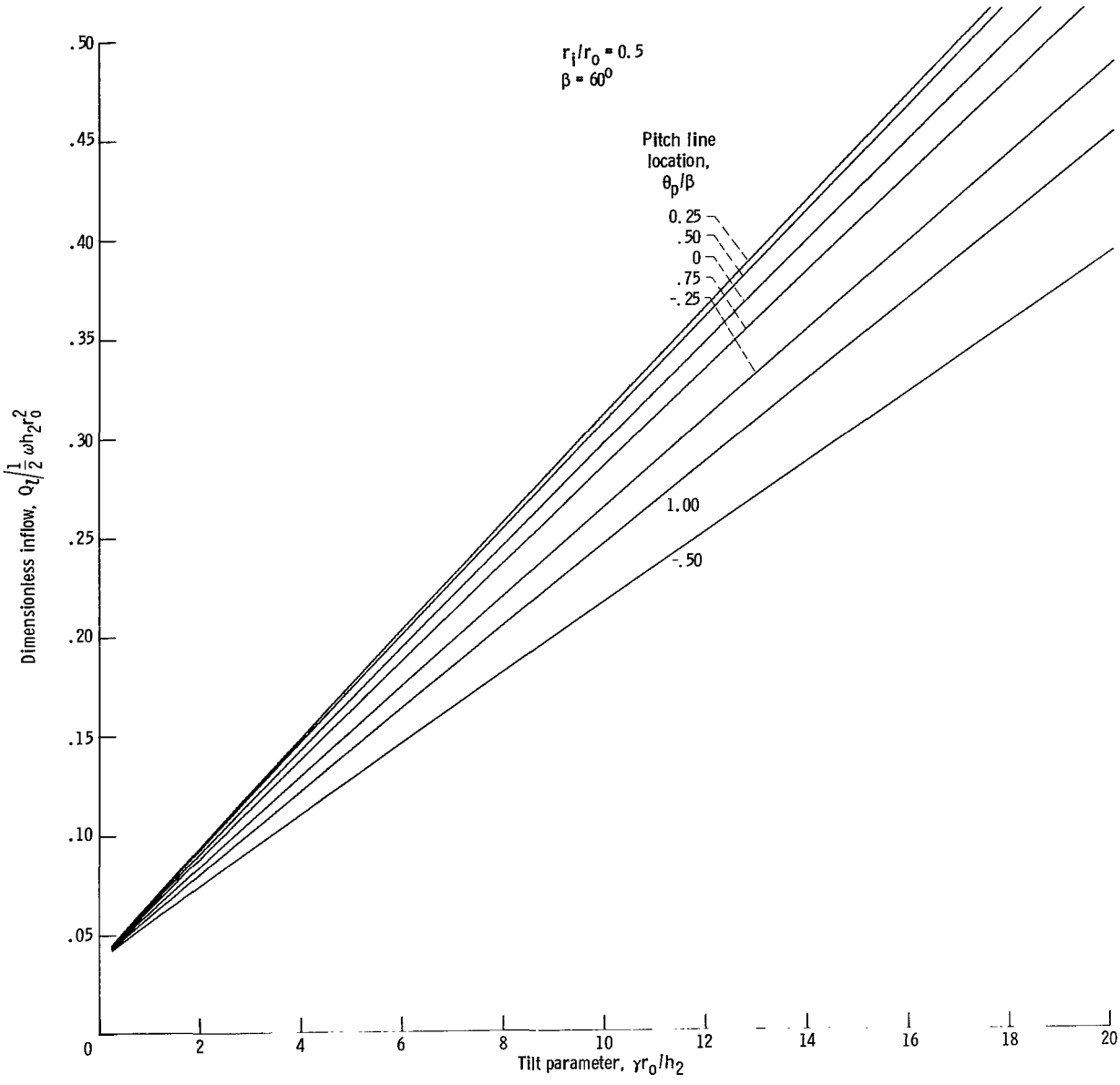

(d) Lubricant inflow.

Figure 8. - Continued.

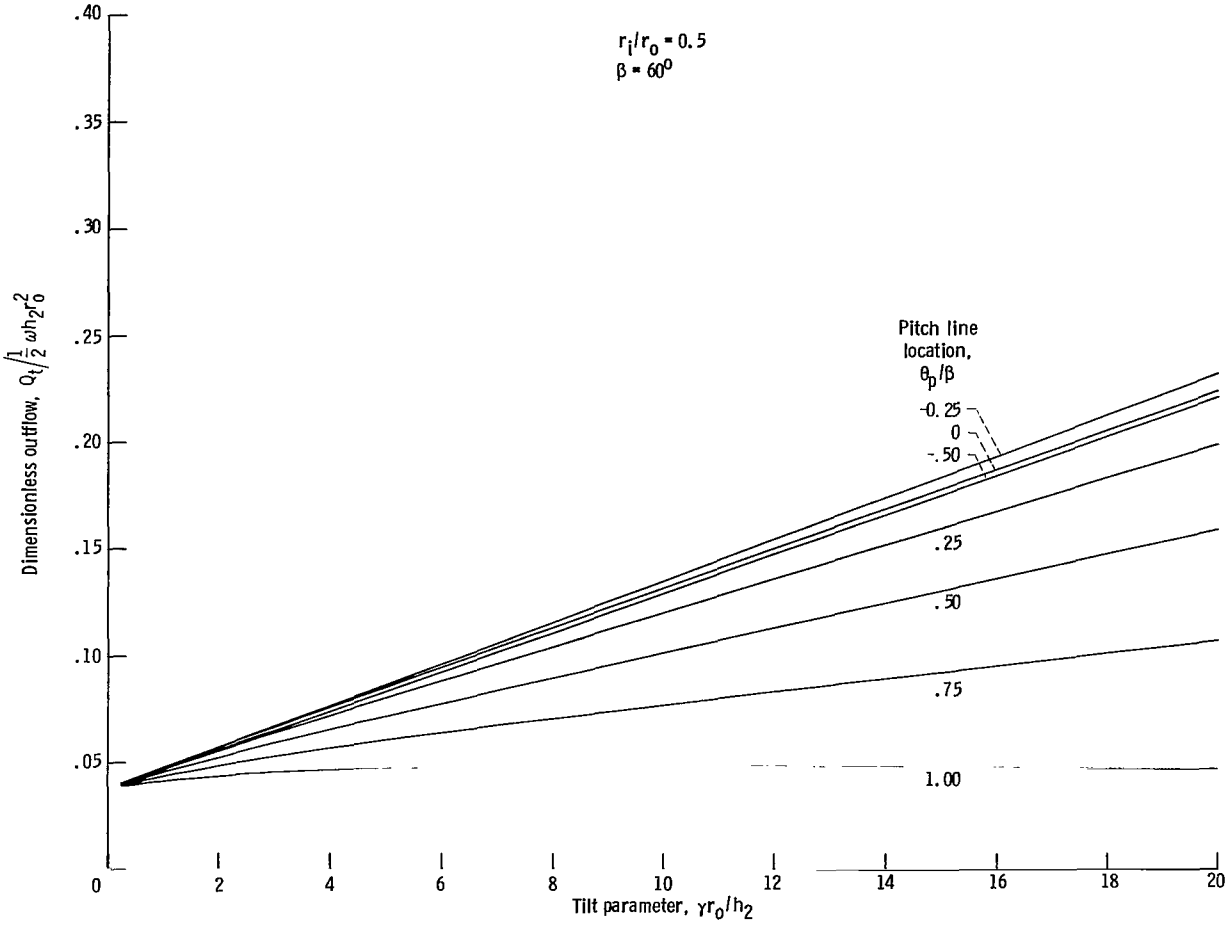

(e) Lubricant outflow at trailing edge.

Figure 8. - Concluded.

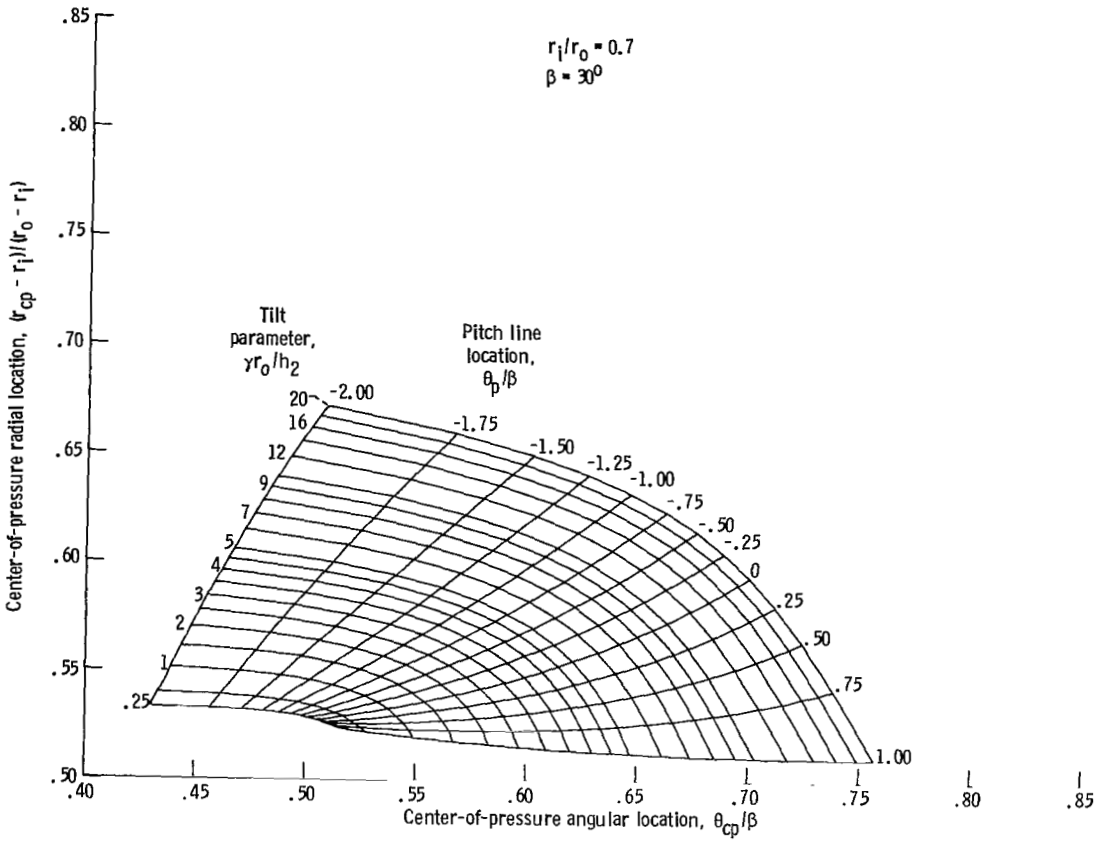

(a) Center of pressure.

Figure 9. - Design charts for flat, sector-shaped pad with ratio of inner to outer radius r_i/r_o of 0.7 and angular extent β of 30^0.

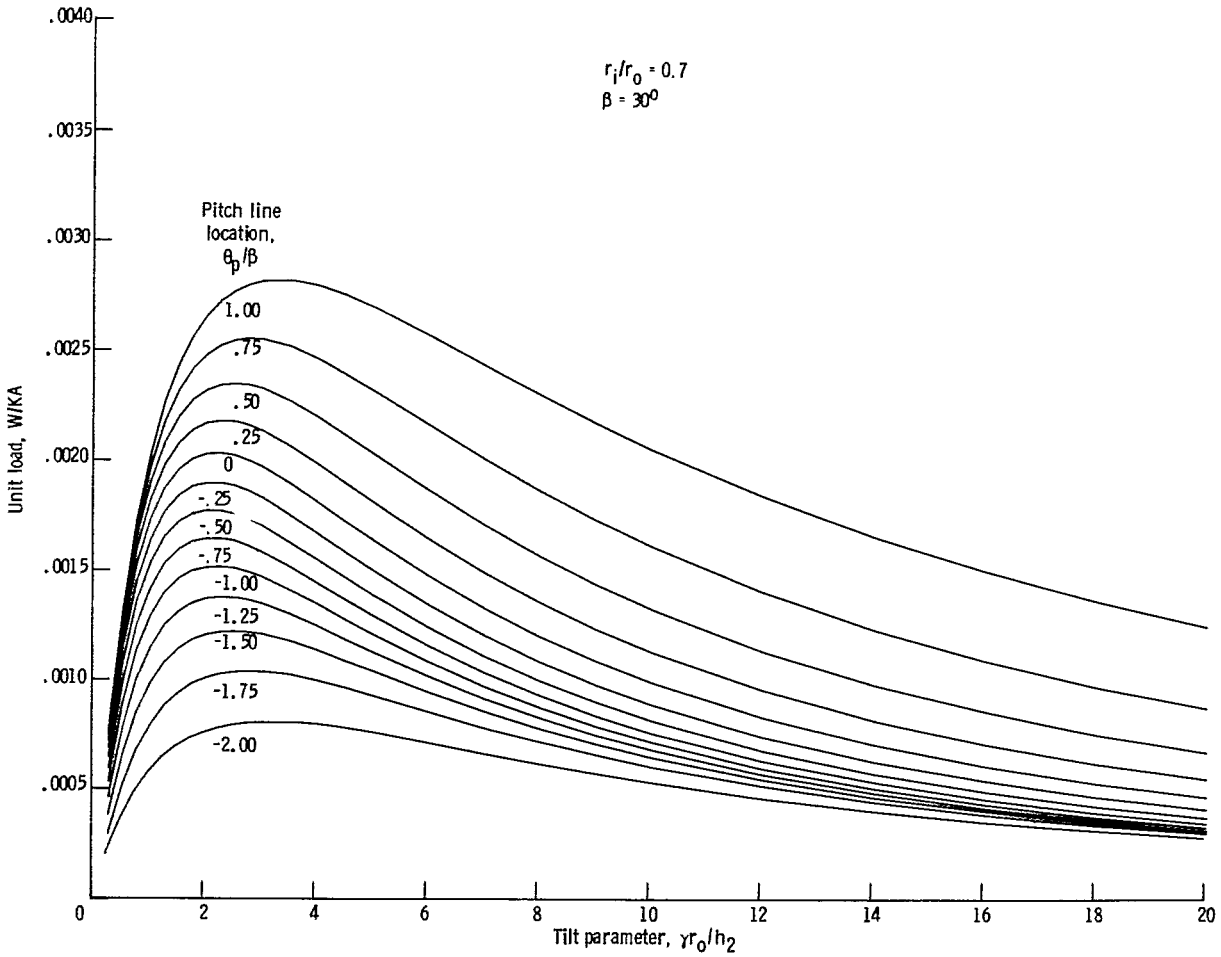

(b) Load capacity.

Figure 9. - Continued.

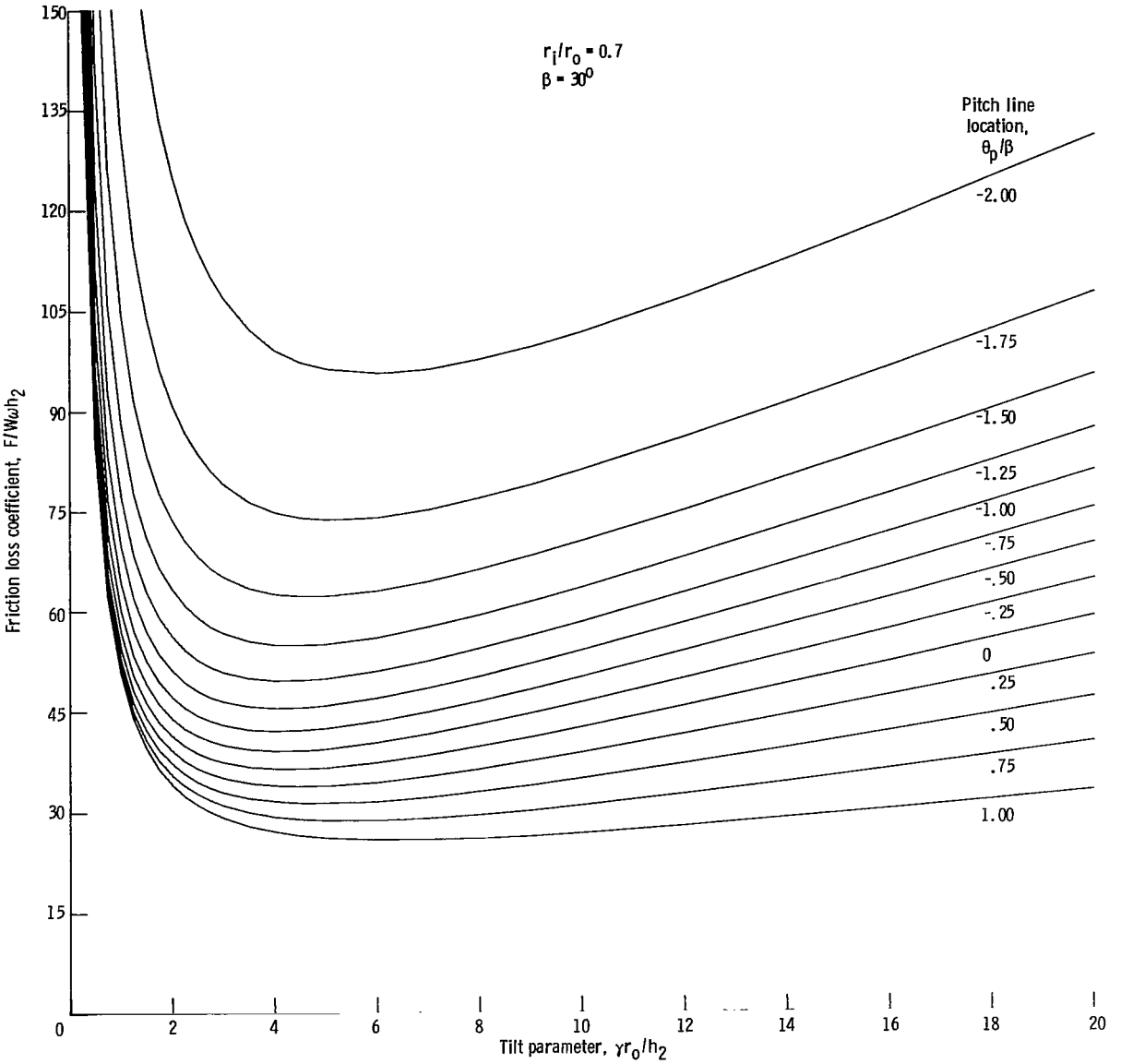

(c) Friction loss.

Figure 9. - Continued.

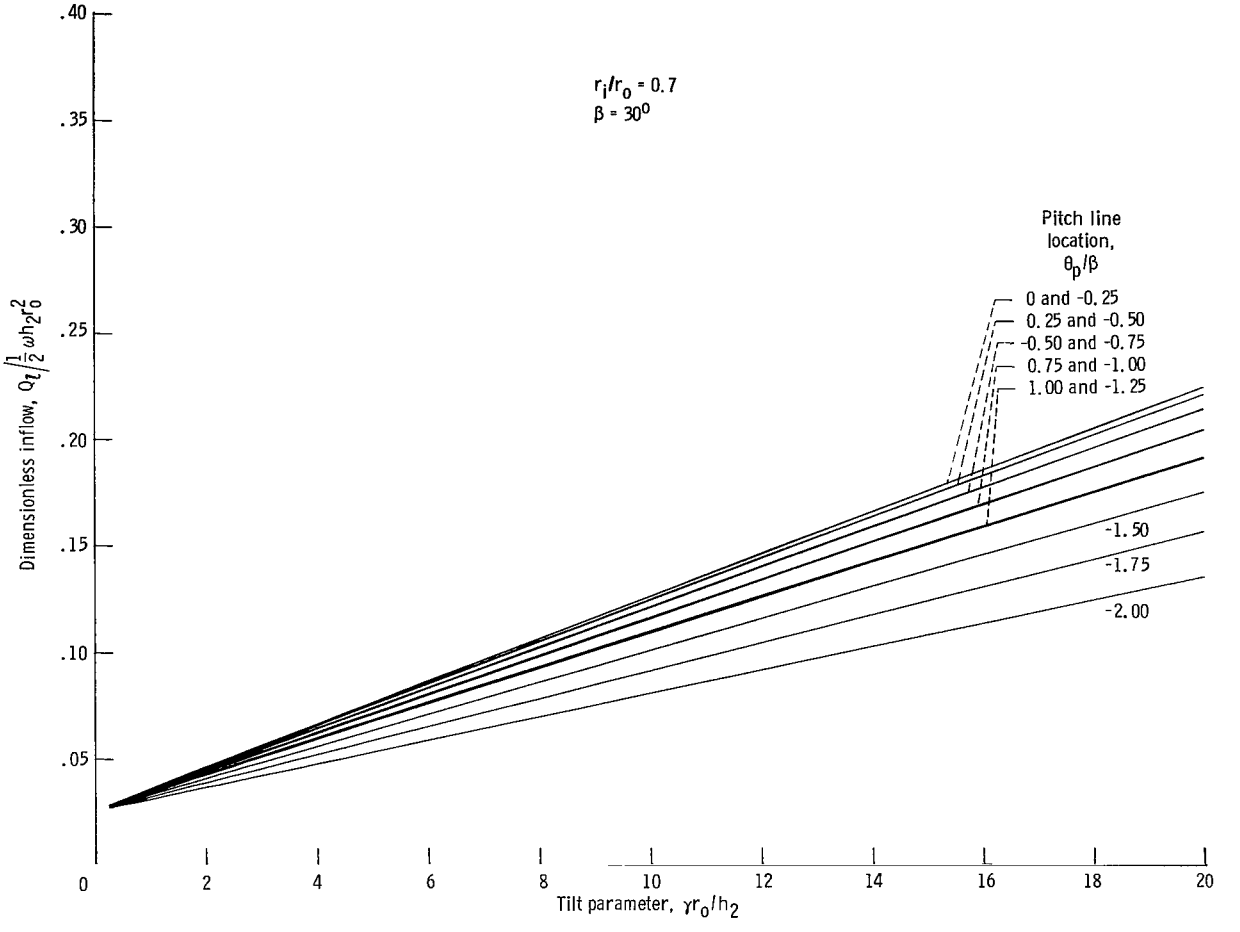

(d) Lubricant inflow.

Figure 9. - Continued.

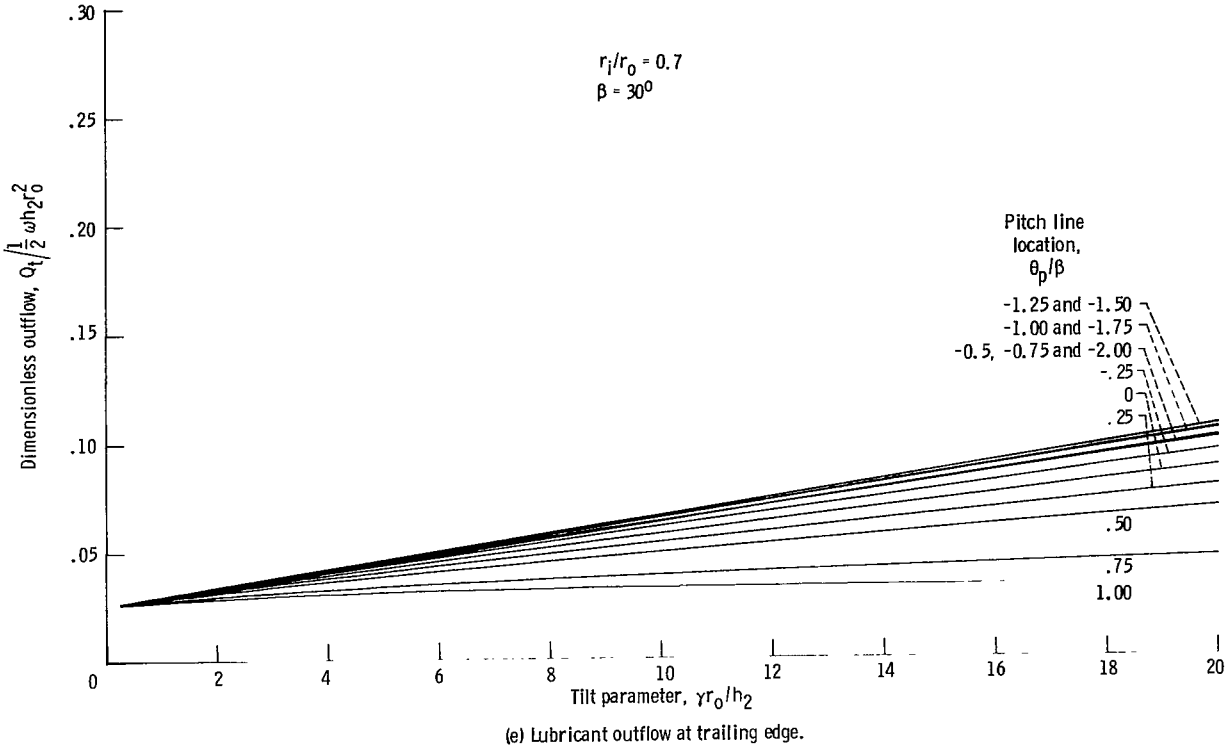

(e) Lubricant outflow at trailing edge.

Figure 9. - Concluded.

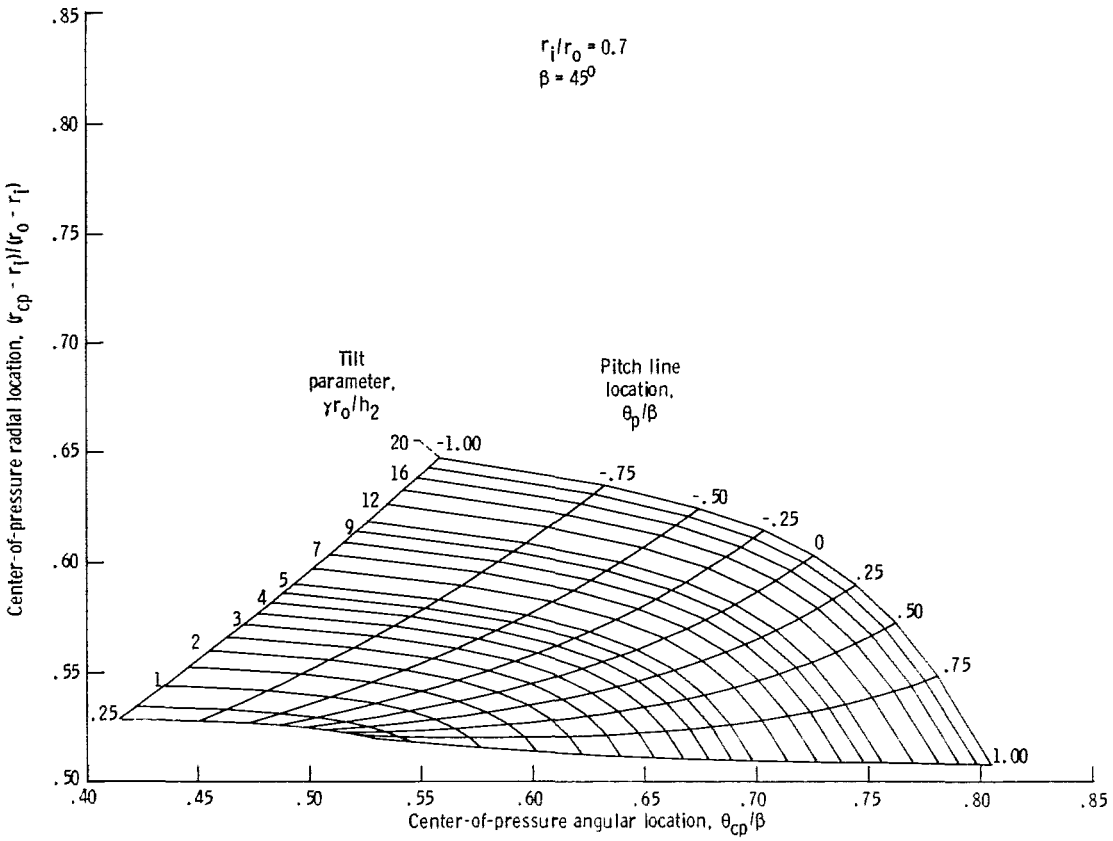

(a) Center of pressure.

Figure 10. - Design charts for flat, sector-shaped pad with ratio of inner to outer radius r_i/r_o of 0.7 and angular extent β of 45^0.

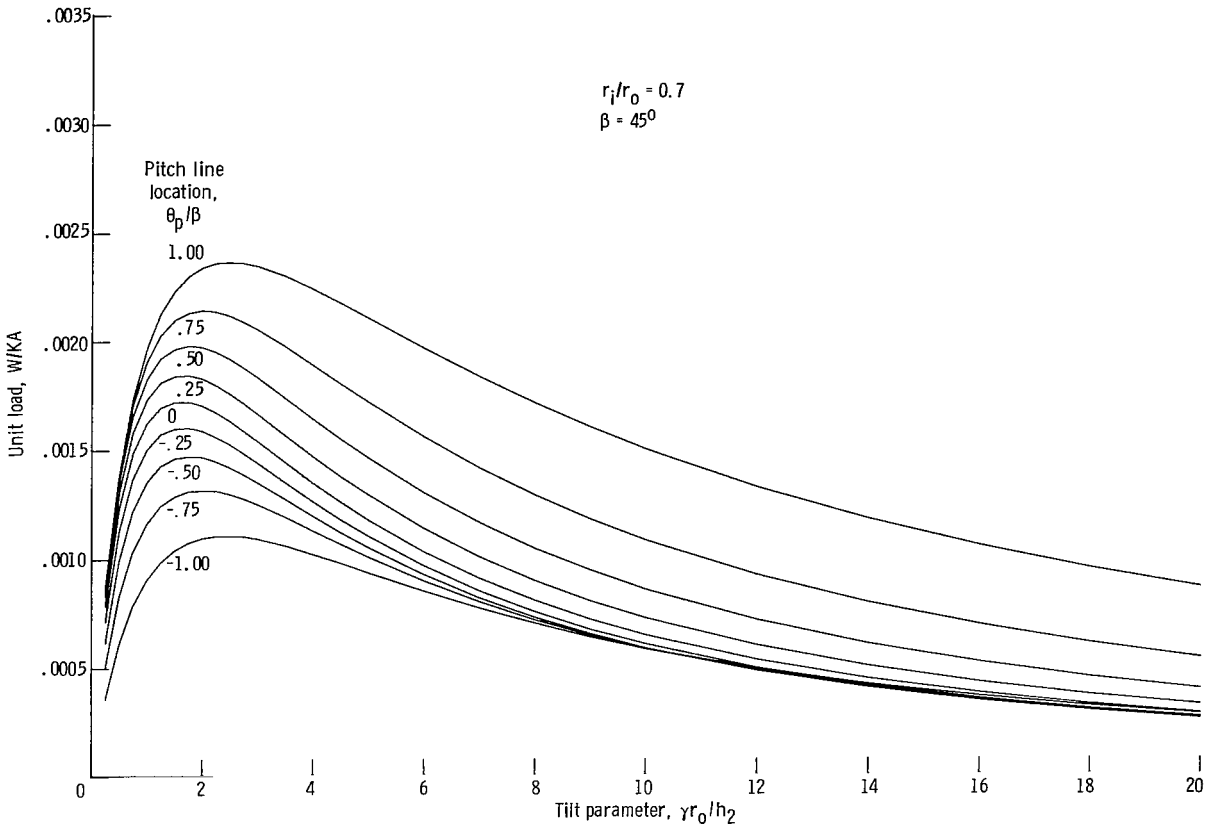

(b) Load capacity.

Figure 10. - Continued.

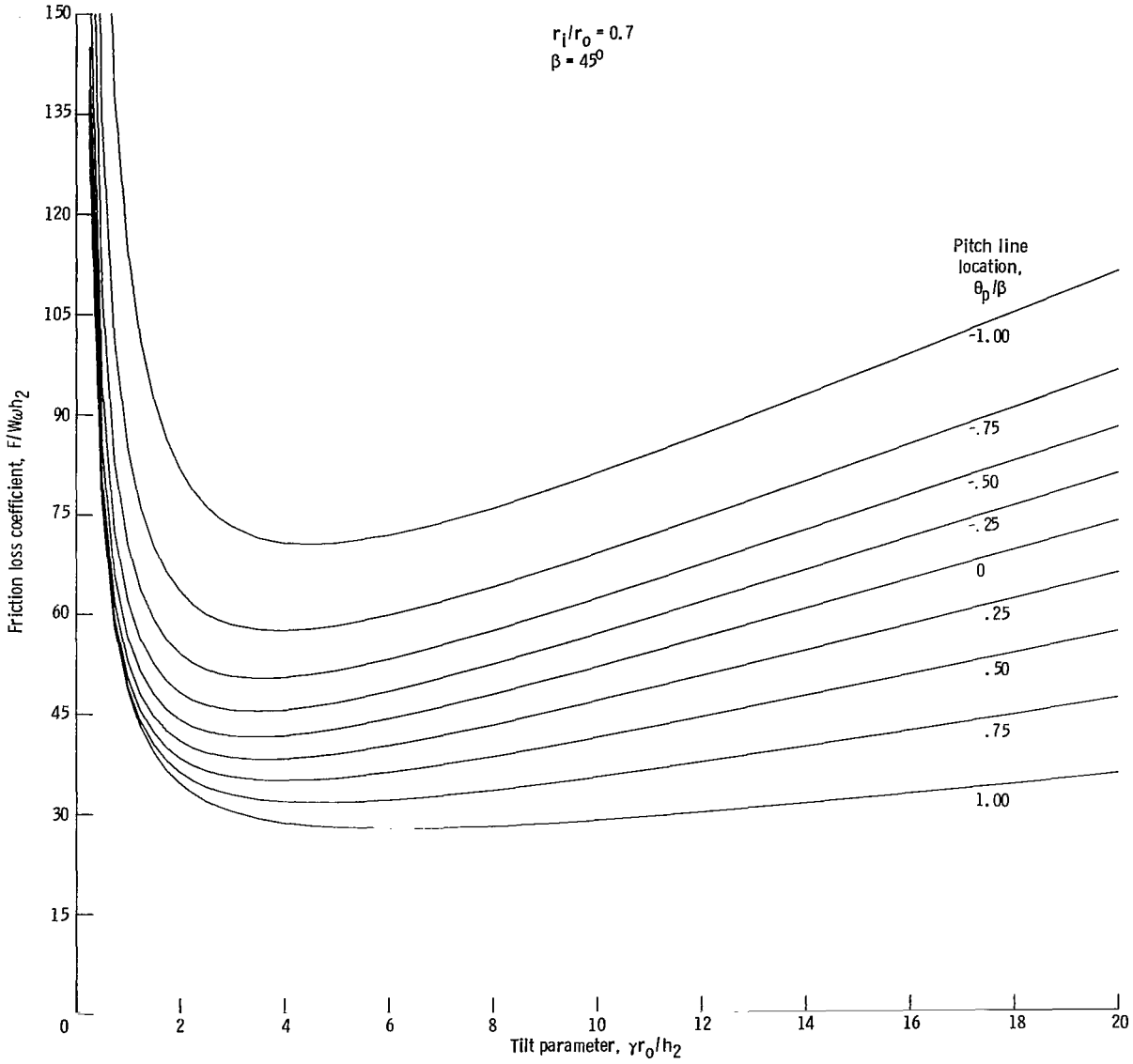

(c) Friction loss.

Figure 10. - Continued.

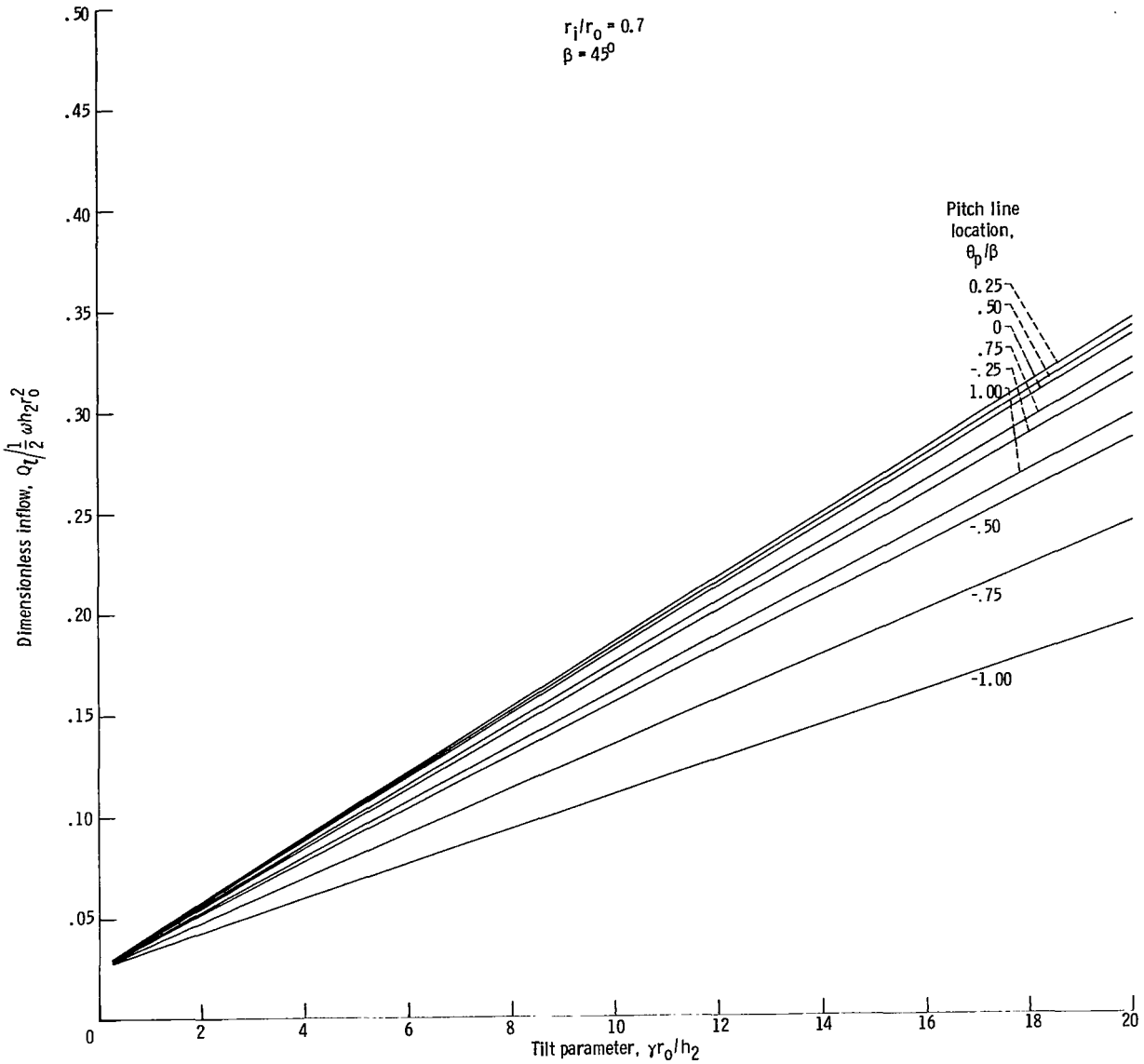

(d) Lubricant inflow.

Figure 10. - Continued.

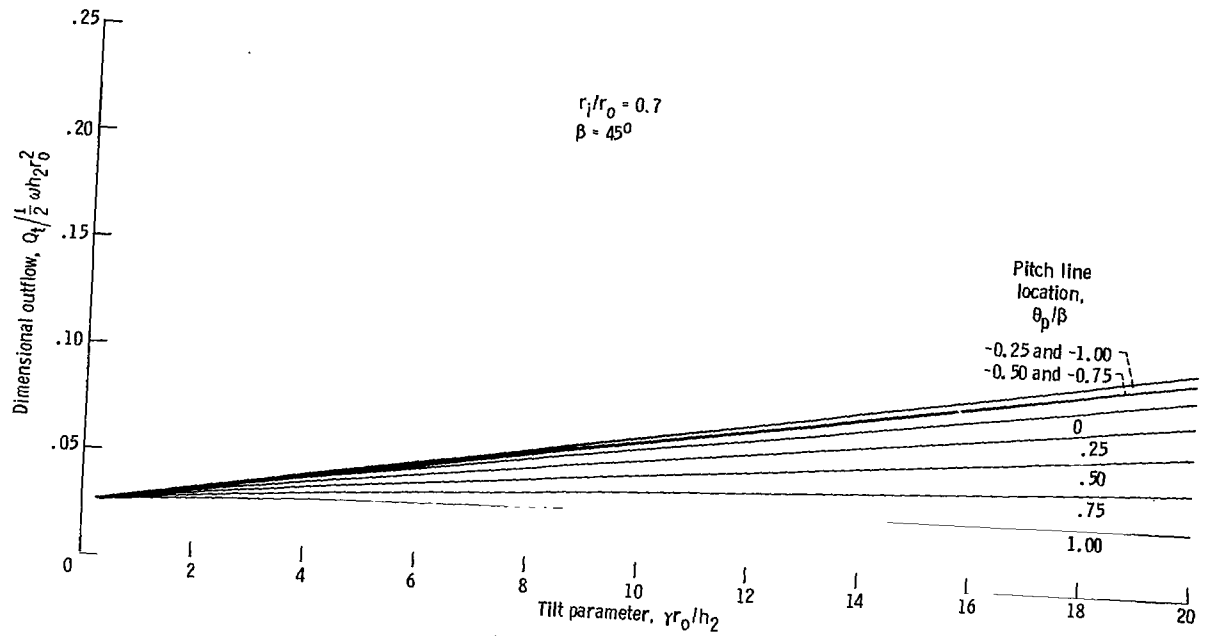

(e) Lubricant outflow at trailing edge.

Figure 10. - Concluded.

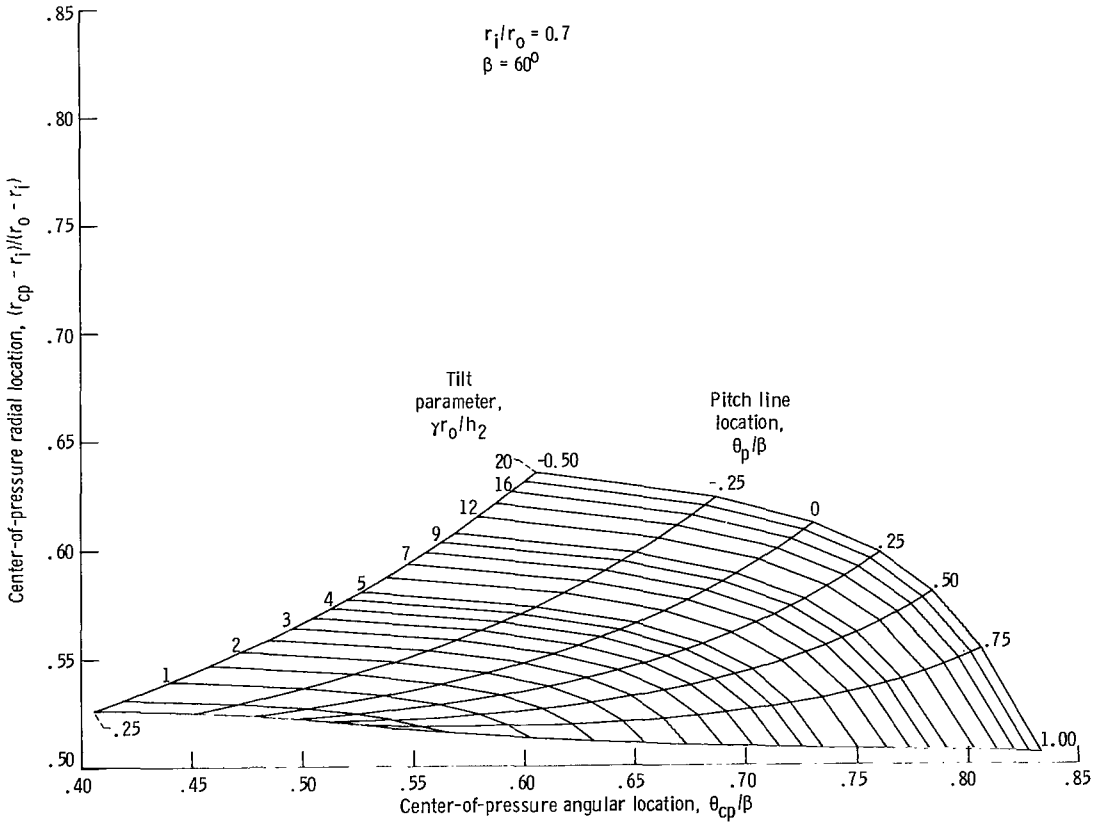

(a) Center of pressure.

Figure 11. - Design charts for flat, sector-shaped pad with ratio of inner to outer radius r_i/r_o of 0.7 and angular extent β of 60^o.

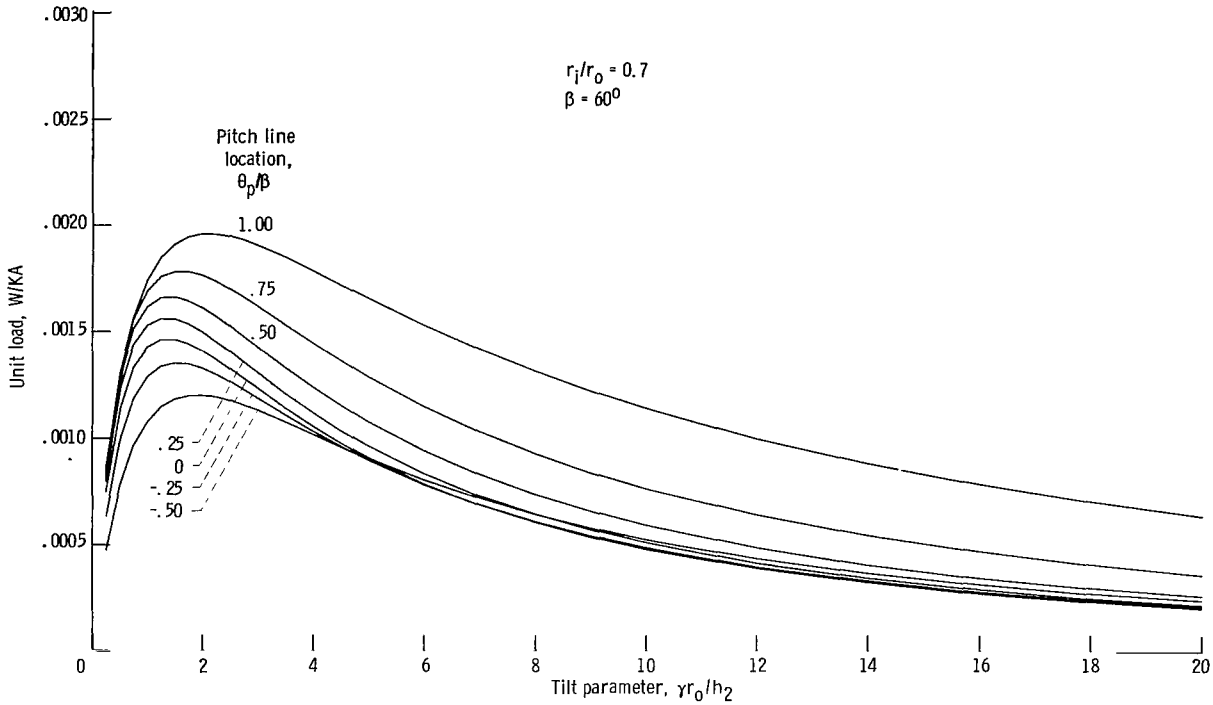

(b) Load capacity.

Figure 11. - Continued.

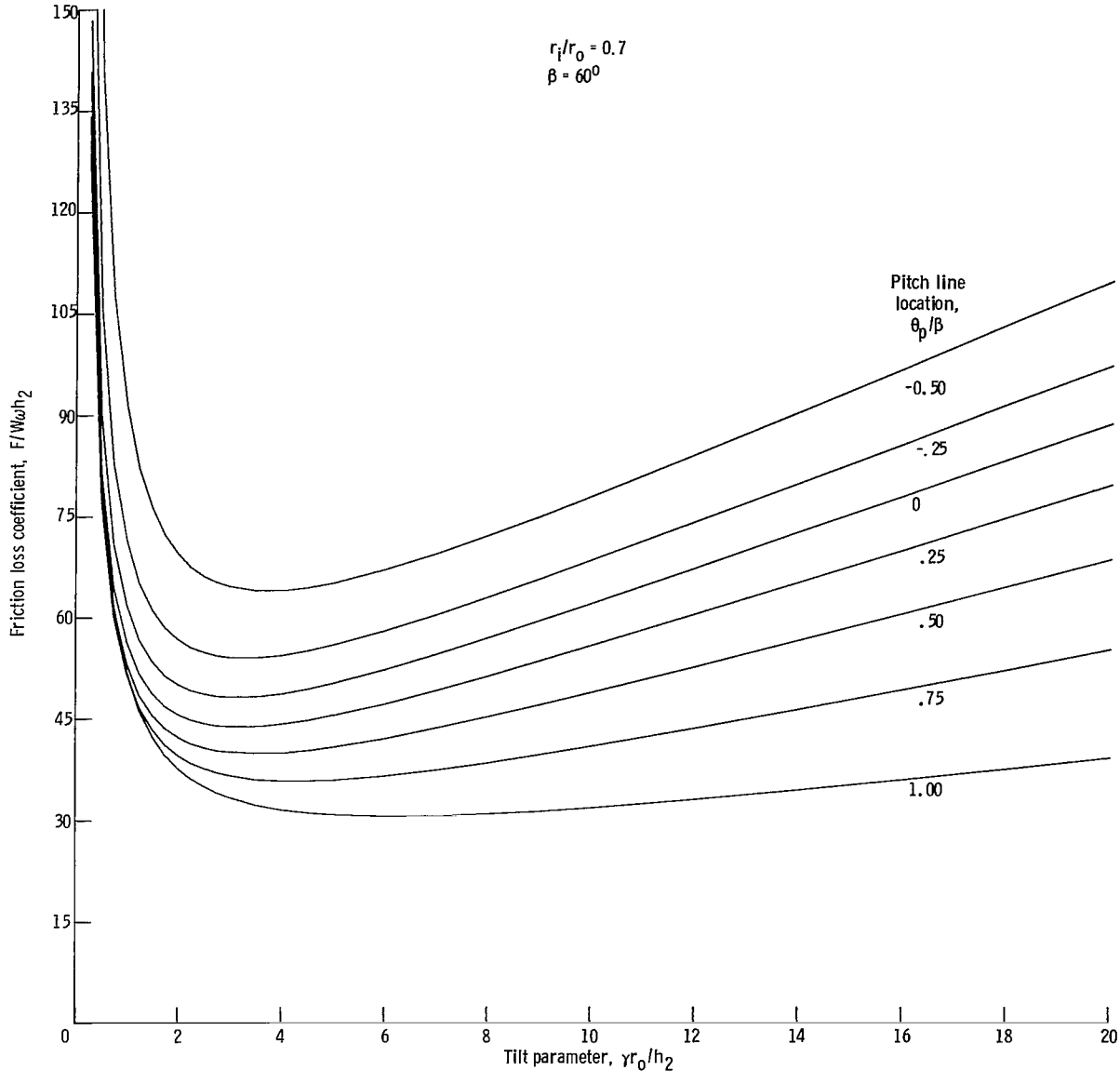

(c) Friction loss.

Figure 11. - Continued.

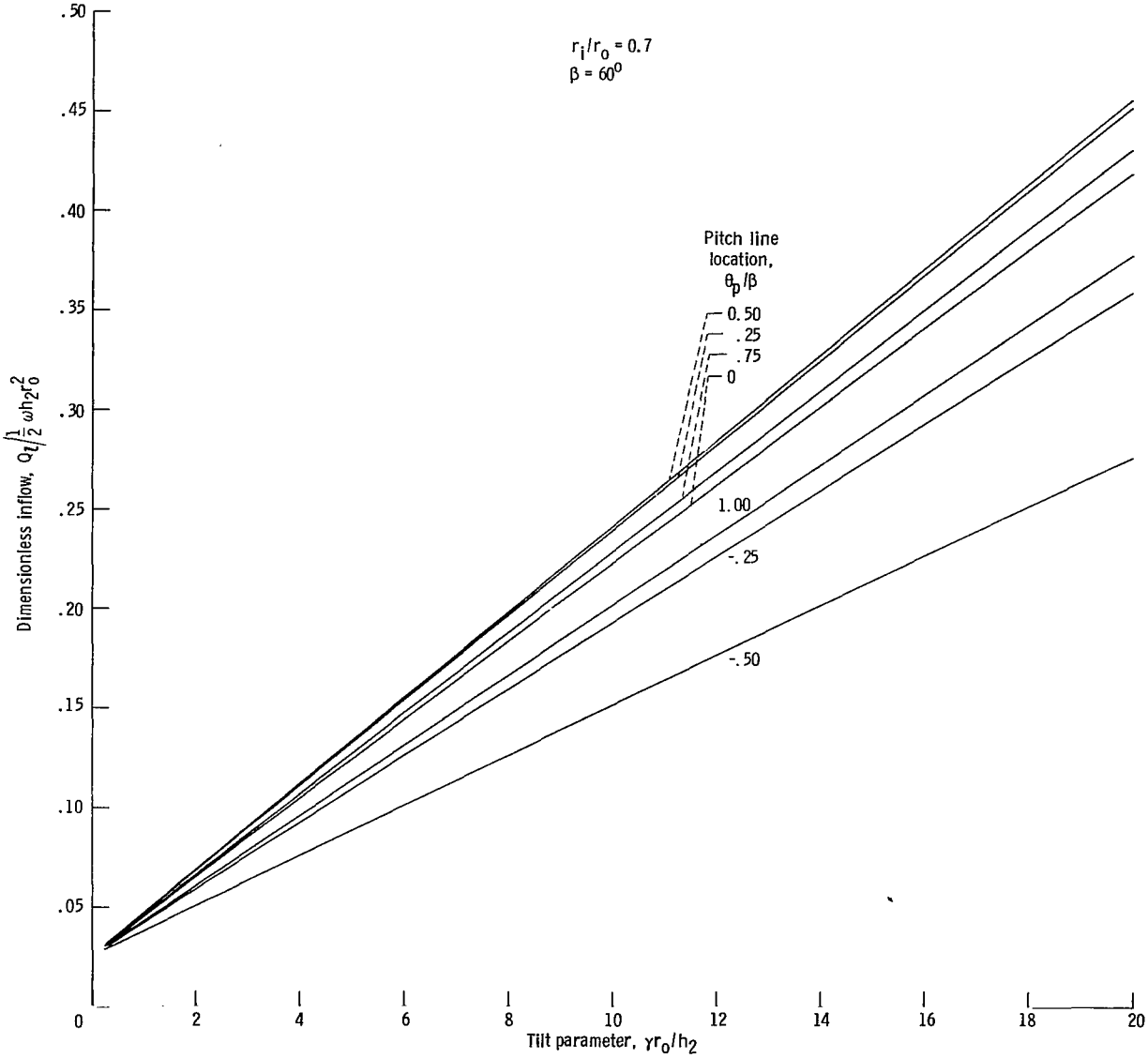

(d) Lubricant inflow.

Figure 11. - Continued.

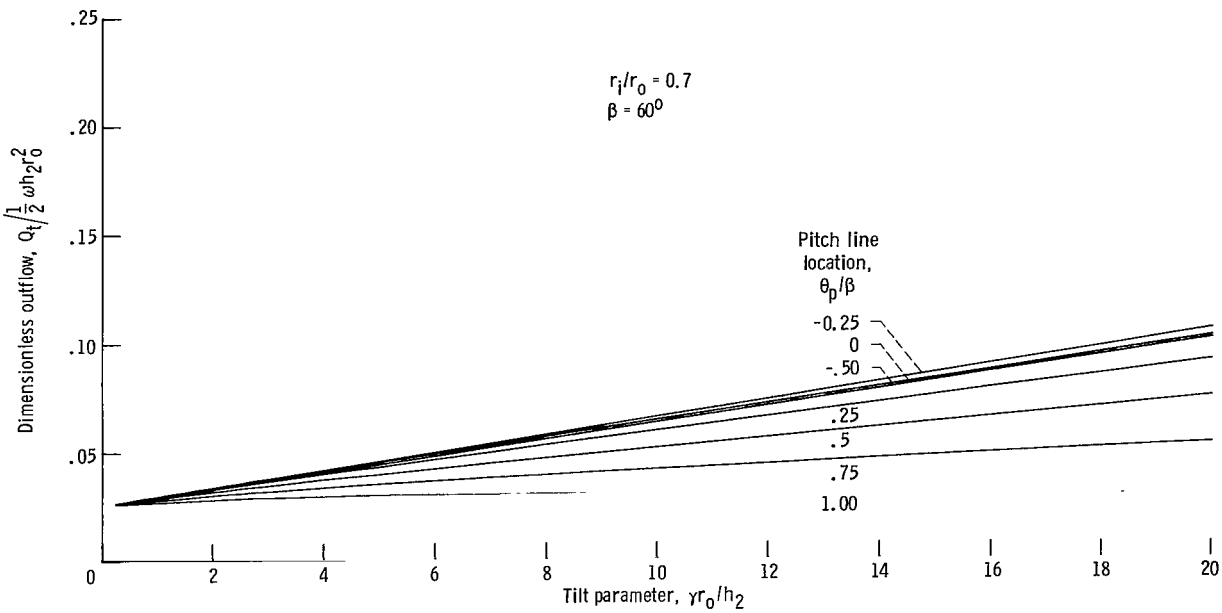

(e) Lubricant outflow at trailing edge.

Figure 11. - Concluded.

256 001 C1 U D 770325 S00903DS
DEPT OF THE AIR FORCE
AF WEAPONS LABORATORY
ATTN: TECHNICAL LIBRARY (SUL)
KIRTLAND AFB NM 87117

"The aeronautical and space activities of the United States shall be conducted so as to contribute . . . to the expansion of human knowledge of phenomena in the atmosphere and space. The Administration shall provide for the widest practicable and appropriate dissemination of information concerning its activities and the results thereof."

—NATIONAL AERONAUTICS AND SPACE ACT OF 1958

NASA SCIENTIFIC AND TECHNICAL PUBLICATIONS

TECHNICAL REPORTS: Scientific and technical information considered important, complete, and a lasting contribution to existing knowledge.

TECHNICAL NOTES: Information less broad in scope but nevertheless of importance as a contribution to existing knowledge.

TECHNICAL MEMORANDUMS: Information receiving limited distribution because of preliminary data, security classification, or other reasons. Also includes conference proceedings with either limited or unlimited distribution.

CONTRACTOR REPORTS: Scientific and technical information generated under a NASA contract or grant and considered an important contribution to existing knowledge.

TECHNICAL TRANSLATIONS: Information published in a foreign language considered to merit NASA distribution in English.

SPECIAL PUBLICATIONS: Information derived from or of value to NASA activities. Publications include final reports of major projects, monographs, data compilations, handbooks, sourcebooks, and special bibliographies.

TECHNOLOGY UTILIZATION PUBLICATIONS: Information on technology used by NASA that may be of particular interest in commercial and other non-aerospace applications. Publications include Tech Briefs, Technology Utilization Reports and Technology Surveys.

Details on the availability of these publications may be obtained from:

SCIENTIFIC AND TECHNICAL INFORMATION OFFICE

NATIONAL AERONAUTICS AND SPACE ADMINISTRATION

Washington, D.C. 20546